https://doi.org/10.5194/egusphere-2026-1165
Preprint. Discussion started: 6 May 2026

Experiment design, nudging protocol, and models participating in Phase 2 of the APARC Quasi-Biennial Oscillation initiative (QBOi)

James A. Anstey[1], Neal Butchart[2], Scott Osprey[3], Yoshio Kawatani[4], Kevin Hamilton[5], Jadwiga H. Richter[6], Tim Stockdale[7], Martin B. Andrews[2], Zhaoyang Chai[8], Paolo Davini[9], Dong-Chan Hong[10], Kai Huang[6], Aleena M. Jaison[3], Tobias Kerzenmacher[11], Jeff R. Knight[2], Pu Lin[12], Francois Lott[13], Yixiong Lu[14], Hiroaki Naoe[15], Federico Serva[16], Isla Simpson[6], Seok-Woo Son[10], Qi Tang[17], Shingo Watanabe[18,19], Jinbo Xie[17,20], and Kohei Yoshida[15]

[1]Canadian Centre for Climate Modelling and Analysis (CCCma), Victoria, Canada
[2]Met Office Hadley Centre (MOHC), Exeter, UK
[3]National Centre for Atmospheric Science (NCAS), University of Oxford, Oxford, UK
[4]Faculty of Environmental Earth Science, Hokkaido University, Sapporo, Japan
[5]International Pacific Research Center (IPRC), Honolulu, USA
[6]National Center for Atmospheric Research (NCAR), Boulder, USA
[7]European Centre for Medium-Range Weather Forecasts (ECMWF), Reading, UK
[8]Institute of Atmospheric Physics, Chinese Academy of Sciences (CAS), Beijing, China
[9]Institute of Atmospheric Sciences and Climate, National Research Council (CNR-ISAC), Torino, Italy
[10]School of Earth and Environmental Sciences, Seoul National University, Seoul, 08826, Korea
[11]Karlsruher Institut für Technologie (KIT), Karlsruhe, Germany
[12]Atmospheric and Oceanic Sciences, Princeton University, Princeton, USA
[13]Laboratoire de Météorologie Dynamique (LMD), Paris, France
[14]Earth System Modeling and Prediction Centre, China Meteorological Administration (CMA), Beijing, China
[15]Meteorological Research Institute (MRI), Tsukuba, Japan
[16]Institute of Marine Sciences, National Research Council (CNR-ISMAR), Rome, Italy
[17]Lawrence Livermore National Laboratory, Livermore, CA, USA)
[18]Japan Agency for Marine-Earth Science and Technology (JAMSTEC), Yokohama, Japan
[19]Advanced Institute for Marine Ecosystem Change (WPI-AIMEC, Tohoku University, Sendai, Japan)
[20]High Meadows Environmental Institute (HMEI), Princeton University, Princeton, NJ, USA

Correspondence: James Anstey (james.anstey@ec.gc.ca)

Abstract.

We describe the protocol for coordinated experiments in phase-2 of the Quasi-Biennial Oscillation initiative (QBOi) and the participating models. The experiments involve nudging tropical stratospheric zonal-mean zonal winds in the models toward observations, enabling analysis of the impact of QBO biases on simulated teleconnections. Additionally, nudging the tropical winds allows investigation of the origins of QBO biases by examining the behaviour of resolved and parameterized equatorial waves under realistic equatorial wind shear conditions. We document here the scientific rationale and design of the nudging experiments, summarize the QBOi data request, and provide an overview of participating models. An initial evaluation is given of tropical stratospheric winds simulated by the multi-model ensemble for both nudged and free-running cases, and the overall impact of nudging on climatological aspects of the atmospheric circulation is examined.

https://doi.org/10.5194/egusphere-2026-1165
Preprint. Discussion started: 6 May 2026

1 Introduction

The ability of climate models to simulate the quasi-biennial oscillation (QBO) of tropical stratospheric winds has long been viewed as a potential additional source of predictive skill on subseasonal to decadal timescales (Baldwin et al., 2001; Hoskins, 2013; Butchart, 2022; Scaife et al., 2022). Accurate simulation of the QBO has proved challenging (e.g., Schenzinger et al., 2017) due primarily to the QBO's strong sensitivity to model horizontal and vertical resolutions, and the parameterization of physical processes such as deep convection and non-orographic gravity wave drag. Consequently, simulated QBOs often have large biases. Without a reduction in these biases improvements in the predictive skill resulting from QBO teleconnections may not be possible. Likewise, QBO impacts on transport, important in chemistry-climate model simulations, may not be accurately simulated in models with large QBO biases. To address challenges in modelling the QBO the Atmospheric Processes And their Role in Climate (APARC)[1] Quasi-Biennial Oscillation initiative (QBOi) was proposed (Anstey et al., 2022a).

For the fifth phase of the Coupled Model Intercomparison Project (CMIP5), only a few of the participating models could simulate the QBO, even among those that were stratosphere-resolving with relatively high upper boundaries at 1 hPa or above (Butchart et al., 2018). As the number of models capable of simulating QBO-like oscillations increased, the possibility of a multi-model comparison to better understand the causes of model biases and inter-model differences in simulating the QBO emerged. Hence phase-1 of QBOi was launched in 2015 with community agreement on the design of a set of five coordinated experiments (Hamilton et al., 2015) to be performed by Atmospheric General Circulation Models (AGCMs) using identical prescribed sea surface temperatures (SSTs), sea ice (SI) and other external forcings. These included idealized present-day and future experiments, and a set of hindcasts to assess QBO predictability (Butchart et al., 2018). An extension of phase-1 examined the impact of idealized El Niño and La Niña tropical SST conditions on the QBO (Kawatani et al., 2025) and on interactions between the El Niño-Southern Oscillation (ENSO) teleconnections and QBO teleconnections (Naoe et al., 2025), and between the QBO and the Madden-Julian Oscillation (MJO, Elsbury et al., 2025).

A key finding from QBOi phase-1 was that the multi-model ensemble of simulated QBOs tended to show similar biases, including underestimated amplitude at the lower altitudes of the QBO around 50 hPa ($\sim$ 21 km), particularly in the strength of the easterly QBO phase (Bushell et al., 2022). Model shortcomings in predicting QBO evolution from initial conditions (Stockdale et al., 2022) and in simulating QBO teleconnections (Anstey et al., 2022b) are likely related to these common biases. Meanwhile, complementary analysis of CMIP6 simulations showed that while many more participating models could simulate a QBO compared to CMIP5, the QBO biases in CMIP6 models had, on average, not improved compared to phase-1 QBOi models or QBO-resolving models from CMIP5 (Richter et al., 2020). Therefore, despite general progress in climate model development including increased spatial resolution and better resolved stratospheres, and with more QBO-resolving models in CMIP6 than previous CMIP phases, there is still work to do on improving the fidelity of QBO simulations. Uncertainty remains over the vertical resolution required in the tropical lower stratosphere to represent the propagation and damping of resolved waves and how the spectrum of these tropical waves depends on horizontal resolution and parameterized deep convection. The

[1] https://www.aparc-climate.org/, previously the Stratosphere-troposphere Processes and their Role in Climate (SPARC) a core project of the World Climate Reaserch Programme.

https://doi.org/10.5194/egusphere-2026-1165
Preprint. Discussion started: 6 May 2026

essential ingredients needed for non-orographic gravity wave drag parameterizations to accurately represent mean-flow driving by unresolved small-scale tropical waves also remains uncertain. Progress in simulating the QBO is likely to follow from a better understanding of these modeling uncertainties, and improved observational constraints to inform modeling choices (e.g., Bramberger et al., 2023; Lott et al., 2024).

Phase-2 of QBOi is designed to assess how common QBO biases are impacting on the QBO's wave-driving and its teleconnections across a multi-model ensemble. The underlying methodology is to bias-correct the simulated QBO by nudging or relaxing a model's zonal winds in the tropical stratosphere toward reanalysis winds in the same region. To avoid any spurious damping (or exciting) of waves that contribute to the QBO's evolution or its teleconnections to other parts of the atmosphere, only the zonal-mean component of the winds is nudged, provided this is possible within a model's configuration. The impact of QBO biases is investigated through comparison with results from simulations that are identical apart from the absence of the nudging (these simulations then typically have internally generated QBOs), and also with results from a third experiment in which the tropical stratosphere is nudged toward the reanalysis climatology instead of the evolving winds (i.e., the reanalysis QBO). Conceptually the zonal-mean nudging technique used in QBOi phase-2 is similar to that used in the Stratospheric Network for the Assessment of Predictability (SNAP) Stratospheric Nudging And Predictable Surface Impacts (SNAPSI) project for investigating the role of stratospheric polar vortex disturbances in subseasonal to seasonal forecasts (Hitchcock et al., 2022).

The purpose of this paper is to provide an overview of the protocol for the phase-2 experiments including brief motivation for the design choices (Section 2 and Appendices). Common diagnostic output is requested (Section 3) to facilitate the analysis and model comparison. Twelve models are participating in QBOi phase-2 (Section 4). For the nudging protocol to be effective in each of these models it is confirmed in Section 4.2 that in the tropical stratosphere the expected QBO-bias correction of the zonal-mean zonal winds is achieved while in the extra-tropics the nudging has no significant direct or undesired impact on the model's climate (background state). Concluding remarks are presented in Section 5.

2 Experiments

This section provides an overview and scientific rationale for the design of the nudging experiments. Full details of the experimental protocol are provided in Appendices A and B.

The experiments used in QBOi phase-2 are based on the AGCM Experiment 1 (**Exp1**) used in QBOi phase 1 (Butchart et al., 2018), which in turn was based on the CMIP5 experiment 3.3, alternatively referred to as the "Atmospheric Model Intercomparison Project (AMIP)" experiment (Taylor et al., 2012). In this experiment observed monthly varying SSTs and SI amounts were prescribed for 1 January 1979 to 28 February 2009, as well as contemporaneous external forcings (Butchart et al., 2018). For QBOi phase-2, SSTs, SI and other external forcings are updated to CMIP6 specifications (Eyring et al., 2016), where appropriate, and the experiments extended to 31 December 2020 using extensions of the CMIP6 SSTs and SI timeseries made available by the Program for Climate Model Diagnosis and Intercomparison (PCMDI) (Appendix B). The updated **Exp1** enables the QBOs in the model versions used in phase 2 to be evaluated and provides the control against which the impacts of the nudging in two additional experiments (**Exp1-ObsQBO** and **Exp1-NoQBO**) can be measured.

https://doi.org/10.5194/egusphere-2026-1165
Preprint. Discussion started: 6 May 2026

Table 1. Summary of QBOi phase-2 nudging experiments. The recommended target state is monthly and zonal-mean zonal wind $\overline{u}$ derived from ERA5 reanalysis data produced by the European Centre for Medium-Range Weather Forecasts (Hersbach et al., 2020). The region of the tropical stratosphere over which nudging is applied is shown in Figure 1. **Exp1**, with no nudging, is an update of the same experiment from QBOi phase-1.

Experiment	Nudging target state (tropical stratosphere)	Time period	Ensemble size
Exp1	No nudging	1979-2020	3
Exp1-ObsQBO	Time-evolving ERA5 $\overline{u}$	1979-2020	3
Exp1-NoQBO	Climatological ERA5 $\overline{u}$	1979-2020	3

Exp1-ObsQBO and **Exp1-NoQBO** build on **Exp1** by adding nudging in the tropical stratosphere, where the nudging refers to imposing a relaxation toward a prescribed state as an additional forcing in a model's prognostic equations. The prescribed state will be referred to as the "target state" for the nudging, to avoid confusion with other aspects of the simulations that are prescribed (e.g., SSTs). Table 1 gives an overview of the three experiments. Relaxations of zonal winds in the tropical stratosphere to, either an idealised zonal mean QBO (Hamilton, 1998), or to zonal-mean reanalysis winds (Dall'Amico et al., 2010) have previously been used to impose ersatz QBOs in AGCMs that lacked the ability to spontaneous generate a QBO.

In **Exp1-ObsQBO**, zonal-mean zonal wind in the tropical stratosphere is constrained to follow the observed QBO evolution by nudging it toward the time-evolving monthly-mean zonal-mean zonal wind from reanalysis. The nudging relaxation timescale is 5 days in the tropical stratosphere, using the spatial distribution in altitude (pressure) and latitude shown by the black curves in Figure 1. Because the QBO evolves slowly, the 5-day timescale is considered sufficient to constrain it and is broadly consistent with the relaxation timescales used by Hamilton (1998) and Dall'Amico et al. (2010). In contrast, the 5-day timescale is much longer than the 0.25-day timescale used in the SNAPSI project (cf., black and red lines in Figure 1) where the objective is to bias-correct the daily varying zonal mean zonal winds throughout the stratosphere in seasonal hindcasts (Hitchcock et al., 2022). As already noted, only the zonal-mean component of zonal wind is to be nudged in QBOi phase-2 experiments. This allows waves in the tropical stratosphere to evolve freely while influenced by the constrained (bias corrected) zonal-mean background state. The rationale for nudging only the zonal-mean zonal wind is that the QBO is driven by momentum dissipation from upward propagating waves, while temperature adjusts, via the action of a mean-meridional circulation, to maintain thermal wind balance with the vertical shear of the zonal wind that results from the wave driving (Baldwin et al., 2001; Butchart and Anstey, 2024). The approach used here avoids directly forcing a model's zonal-mean temperature and meridional circulation toward the reanalysis, allowing these fields to dynamically adjust to maintain balance within the model with the zonal wind anomalies that are directly forced by the nudging. Hence the nudging can be viewed as an empirical proxy for the wave forcing that drives the QBO in zonal wind – or more specifically, provides the correction to that wave forcing that would be required for the model to generate a QBO that closely resembles the observed one (i.e., the nudging supplements both the resolved and subgrid-scale (parameterized) wave forcing that is spontaneously generated by the model).

https://doi.org/10.5194/egusphere-2026-1165
Preprint. Discussion started: 6 May 2026

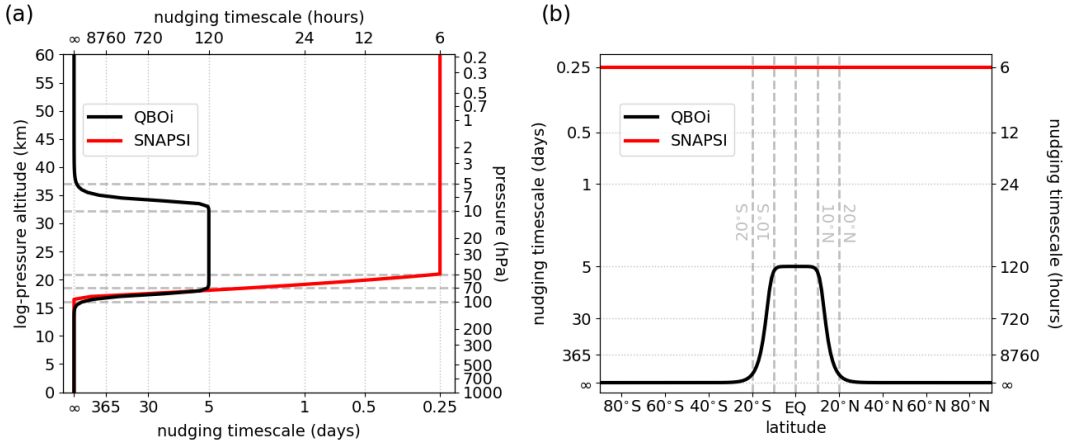

Figure 1. Spatial dependence of nudging timescale in the (a) vertical and (b) meridional directions for the QBOi phase-2 nudging experiments **Exp1-ObsQBO** and **Exp1-NoQBO** (black curves). The mathematical expressions corresponding to the QBOi profiles shown in (a) and (b) are give in Appendix A. Vertical and meridional profiles of nudging timescale from the SNAPSI protocol (Hitchcock et al., 2022) are shown in red for comparison with the QBOi profiles (see Appendix A for further details of the QBOi-SNAPSI comparison).

The chosen vertical nudging profile in Figure 1a indicates that the nudging tapers off from full strength at 70 hPa (~ 18.5 km) to zero at 100 hPa (~ 16 km), near the tropical tropopause, ensuring that upward-propagating waves, generated in the tropical troposphere, propagate upward through increasingly realistic background zonal-mean zonal winds after crossing the tropopause. Extending nudging down to 100 hPa may also be important for determining whether models simulate teleconnections that are thought to be caused by the near-tropopause QBO signal, such as the observed QBO-MJO link (Martin et al., 2021). The nudging profile at full strength extends upward only as far as 10 hPa (~ 32 km), before reducing uniformly to zero by 5 hPa (~ 37 km). Radiosondes only provide observations of tropical winds at altitudes up to about 10 hPa, and above this the tropical zonal winds in reanalyses become more uncertain due to the lack of direct observational constraints (Kawatani et al., 2016). Hence the nudging is restricted to altitudes at which there is high confidence in the ability of reanalyses to represent the QBO. Additionally, this choice allows model simulations of the semi-annual oscillation (SAO) to be examined under conditions in which realistic QBO winds filter the equatorial waves that propagate upward into the region above 10 hPa where zonal-mean zonal wind variability is dominated by the SAO.

Similarly, the latitudinal extent of nudging shown in Figure 1b does not span the entire tropical belt of 30°S–30°N. The observed latitudinal profile of QBO wind amplitude is approximately symmetric about the equator with a Gaussian shape having half-maximum values at about 12°S and 12°N (Dunkerton and Delisi, 1985; Butchart and Anstey, 2024). The latitudinal extent of nudging (Figure 1b) is chosen to be strong between these latitudes of half-maximum wind amplitude, tapering off rapidly outside this range. This is consistent with the equatorial width of the wave-driving of the zonal wind QBO (Bushell et al., 2022; Holt et al., 2022) and reduces the risk of the nudging directly impacting zonal-mean zonal wind anomalies outside this region that may result from QBO-teleconnections or the induced mean meridional circulation. Again, the latitudinal extent

https://doi.org/10.5194/egusphere-2026-1165
Preprint. Discussion started: 6 May 2026

of the nudging described here is not too dissimilar from that used in the earlier studies of Hamilton (1998) and Dall'Amico et al. (2010).

Exp1-NoQBO uses the same nudging profiles as **Exp1-ObsQBO** (Figure 1), but the target state for this experiment is the climatological monthly zonal-mean zonal wind state derived from reanalysis, i.e., the climatology of the target state used in **Exp1-ObsQBO**. This removes almost all interannual variability in zonal-mean zonal wind from the nudged region. Nonetheless, because of the asymmetry between the eastward and westward QBO phases the target (climatological) zonal-mean zonal equatorial winds in **Exp1-NoQBO** are only close to zero in the lower stratosphere and are westward above ∼50 hPa (see Section 4.2). Comparison of **Exp1-NoQBO** with **Exp1-ObsQBO** allows assessment of the overall impacts in a model of realistic tropical stratospheric variability (noting that the two experiments have the same climatological tropical stratospheric winds by construction). In turn, the multi-model ensemble provides insight into the robustness of such impacts across different models.

All three experiments should be performed with the same model version, forcings, and boundary conditions. For each experiment, 3 ensemble members of 42 years each (1979–2020 period) are requested (Table 1). This sample size of 126 years for each experiment is considered necessary to reliably diagnose QBO teleconnections in the presence of large sampling variability due to internal atmospheric dynamics (Anstey et al., 2022b) and to more robustly separate QBO impacts from those of ENSO. While this large sample may not be required when analyzing the QBO wave forcing, the 42 years include a wide range of tropical SST conditions, including extreme ENSO phases, that can affect tropical wave generation differently across the models. Also occurring during the 1979–2020 period are the two disruptions to the QBO's regular cycle that were observed during the Northern Hemisphere (NH) winters of 2015/16 and 2019/20, hence the experiments allow the representation of QBO wave driving during these unusual events to be analysed and compared between models and ensemble members. This will provide an indication of the sensitivity of the disruptions to variability or uncertainty in forcing due to waves originating from the extratropics (Newman et al., 2016; Osprey et al., 2016; Anstey et al., 2021).

Since nudging constrains the tropical stratospheric winds, it is not strictly necessary that a model spontaneously simulates the QBO in order to carry out the nudging experiments **Exp1-ObsQBO** and **Exp1-NoQBO**. Additionally, for models in which it is technically not feasible to nudge just the zonal-mean component of the flow, a "full-field" variant of the experiments may be performed in which the local zonal winds are nudged toward local reanalysis winds. The 5-day nudging timescale was chosen as it is sufficiently long to allow short-period equatorial waves to evolve relatively freely when using the full-field nudging, despite some weak direct wave forcing from the nudging. Full details of the nudging implementation (including the full-field variant), forcings and boundary conditions, can be found in Appendices A and B.

3 Data request

The common diagnostic output requested is very similar to QBOi phase-1 (Butchart et al., 2018), with some additional variables. The same set of variables is requested from all experiments. To reduce data volumes, some high-volume variables are requested from only one ensemble member, as described below. Appendix C provides detailed lists of all requested output variables (Tables C1–C6) with a general overview of the data request provided here.

https://doi.org/10.5194/egusphere-2026-1165
Preprint. Discussion started: 6 May 2026

As noted in Butchart et al. (2018), the QBOi data request is primarily based on that of other model intercomparison projects (MIPs), in particular the set of stratospheric dynamical diagnostics requested from CMIP6 simulations by the Dynamics and Variability Model Intercomparison Project (DynVarMIP, Gerber and Manzini, 2016). These include the Transformed Eulerian Mean (TEM) quantities, namely the Eliassen-Palm flux and residual circulation, that allow analysis of the QBO zonal-mean zonal momentum budget. While TEM diagnostics quantify the extent to which the QBO in a model is driven by its resolved flow, a significant fraction of QBO wave driving in most phase-2 models comes from parameterized sub grid-scale waves, and therefore the forcing due to both orographic and non-orographic gravity wave drag parameterizations is also requested. Non-orographic gravity waves have a range of zonal phase speeds and hence can contribute both eastward and westward forcing, directly driving both phases of the QBO. Orographic waves, with zero zonal phase speed, contribute substantially to total wave driving in the extratropical stratosphere and consequently may impact the QBO via their effect on tropical upwelling, which on average opposes the downward propagation of the QBO (Dunkerton, 1997).

The QBOi phase-2 data request also includes the eastward zonal-mean zonal wind tendency due to nudging and to model physics, which were not included in phase-1 (Table C2). These are requested in order to obtain as complete a breakdown of the QBO momentum budget as possible. In **Exp1-ObsQBO**, the time variation of nudging tendency reflects the adjustment a model is making to follow the trajectory of the observed QBO, and in an averaged sense (e.g., composited by QBO phase) it represents the "missing" forcing that would be required for a model to simulate a more realistic QBO. Examining the nudging tendency therefore allows a detailed analysis of biases in QBO driving as a function of altitude, latitude, and QBO phase. The tendency due to model physics is intended to represent contributions from any other sub grid-scale forcings affecting the zonal-mean zonal momentum budget, such as horizontal and vertical diffusivities.

To further analyze QBO wave driving, 3D winds and temperature at 6-hour resolution (instantaneous samples, not time averages) are requested to enable calculation of equatorial wave spectra in a consistent manner across models (Table C5). These are requested on pressure levels so as to facilitate conventional TEM diagnostic calculations (Andrews et al., 1987; Hardiman et al., 2010), but at vertical resolution comparable to (i.e., approximately equivalent to) the spacing between the model levels. High vertical resolution is necessary to prevent loss of information due to vertical interpolation, which can significantly affect estimates of QBO wave driving (Kim and Chun, 2015; Kim et al., 2019). The horizontal grid should be a regular latitude-longitude grid, ideally the native grid, but if not then at a resolution similar to that of the native grid (again, to avoid losing information due to interpolation). To limit data volumes, only the altitude range 150–0.4 hPa ($\sim$ 13–54 km) is requested. This altitude range has been extended downward compared to the phase-1 data request (Butchart et al., 2018, Table 4) to ensure better coverage of the upper troposphere lower stratosphere (UTLS). These diagnostics are requested only for a single ensemble member, which is expected to be sufficient to characterize inter-model differences in QBO wave driving. If further reduction in data volume is necessary, these diagnostics can be optionally excluded outside the latitude band 15°S to 15°N, where wave driving of the QBO occurs (e.g., Holt et al., 2022).

Apart from the 6-hourly data for equatorial wave analysis, most quantities are requested on the same standard set of 30 pressure levels as in phase-1 that provide vertical resolution ranging from 1.0 to 1.5 km in the 200–40 hPa region (Butchart, 2022). A further addition in phase-2 is that 3-hourly precipitation and outgoing longwave radiation (OLR) were requested to

https://doi.org/10.5194/egusphere-2026-1165
Preprint. Discussion started: 6 May 2026

enable analysis of MJO-like behaviour in the models. The same output variables are requested for all ensemble members of all experiments, with the exception that 6-hourly output for equatorial wave analysis is only required for the first ensemble member, in order to limit data volumes. (And nudging tendency is of course only required for nudged experiments.)

The full set of output variables is tabulated in Appendix C (Tables C1–C6) where further details on the output requirements are given. For ease of comparison with the QBOi phase-1 data request (Butchart et al., 2018), Table C7 summarizes all additions and changes to the QBOi data request since phase-1.

4 Models

4.1 Model characteristics

This section gives a brief overview of the participating models. Table 2 lists the models, including the number of ensemble members performed for each experiment, and the nudging methodology used. Information about model horizontal and vertical resolution (Table 3) and non-orographic gravity wave parametrizations (Table 4) is also provided. Comprehensive descriptions of each model can be found in the appropriate model documentation papers (listed in Table 3), and only their salient aspects with regard to the QBO or its teleconnections are described here.

Out of the 12 participating models listed in Table 2, 9 implemented zonal-mean nudging while 3 implemented the full-field variant of the nudging experiments (Appendix A). Models using full-field nudging will to some extent constrain tropical waves to follow the reanalysis data, but the 5-day nudging timescale employed should ameliorate this effect as the highest frequency waves will not be directly constrained by the nudging to any significant extent. In models using zonal-mean nudging, all tropical waves evolve freely and only the zonal-mean wind is constrained to follow the nudging target state (reanalysis zonal-mean zonal wind).

Information on the models' horizontal and vertical resolution is provided in Table 3. The models vary in their method of horizontal discretization, but it should be noted that most have horizontal resolutions that are comparable to CMIP6 climate models. Since the QBO is sensitive to forcing by small-scale tropical waves, all the models apart from GRIMs include parameterized non-orographic gravity wave drag (GWD) to provide additional wave forcing in the tropics. Details of the GWD parameterization schemes used are given in Table 4. The GRIMs model does not spontaneously generate its own QBO and did not preform **Exp1**. Nonetheless as previously noted the absence of a spontaneously generated QBO does not exclude the model from performing and providing useful output for the nudged simulations (**Exp1-ObsQBO** and **Exp1-NoQBO**) in which tropical stratospheric variability results from the nudging.

Many models also parameterize the tropospheric sources of sub grid-scale waves using variability in the model's convective heating or precipitation. References for the different convective parametrization schemes used by the models are given in Table 4. Note that there are two variants (p1, p2) of the MIROC6.1 model that differ only in their convective parameterization scheme and tuning, but are otherwise identical. Parameterized deep convection generates heating in the tropical troposphere that forces equatorial waves with a range of spatial scales and frequencies which then contribute to driving the QBO in the stratosphere (e.g., Holt et al., 2022) The precise details of the tropical wave spectrum forcing the QBO in each model depends on the

https://doi.org/10.5194/egusphere-2026-1165
Preprint. Discussion started: 6 May 2026

Table 2. Participating models, number of ensemble members for each experiment, and model documentation references. The nudging type is indicate as zonal-mean (ZM), in which case only the zonal-mean zonal wind is nudged, or full-field (FF); for further details of the nudging methodology, see Appendix A.

Model	Institute	Exp1	Exp1-ObsQBO	Exp1-NoQBO	Nudging type	Investigator (email)
BCC-CSM2-MR	CMA / CEMC	3	3	3	ZM	Y. Lu (luyx@cma.gov.cn) W. Jie (jiewh@cma.gov.cn) Z. Chai (czy@mail.iap.ac.cn)
CAS-ESM	CAS / IAP	3	3	3	ZM	Z. Chai (czy@mail.iap.ac.cn)
CESM2	NCAR	3	3	3	ZM	Y. Richter (jrichter@ucar.edu) I. Simpson (islas@ucar.edu) N. Rosenbloom (nanr@ucar.edu) K. Huang (huangkai@ucar.edu)
E3SMv2	DOE	3	3	3	FF	Q. Tang (tang30@llnl.gov) J. Xie (jinbo.xie@princeton.edu)
EC-Earth3	EC-Earth Consortium /CNR	1	1	1	FF	F. Serva (federico.serva@artov.isac.cnr.it) P. Davini (paolo.davini@cnr.it)
ESM4	GFDL	3	3	3	FF	P. Lin (pulin@princeton.edu)
GRIMs 4.0	Seoul National University	0 0	1 1	1 1	ZM ZM	S.-W. Son (seokwooson@snu.ac.kr) D.-C. Hong (eaudetint@snu.ac.kr)
HadGEM3GA7.1	MOHC Oxford University	3	3	3	ZM	M. Andrews (martin.andrews@metoffice.gov.uk) N. Butchart (neal.butchart@metoffice.gov.uk) S. Osprey (scott.osprey@physics.ox.ac.uk)
LMDz6	LMD	1	3	2	ZM	F. Lott (flott@lmd.ens.fr), Lionel Guez (guez@lmd.ipsl.fr)
MIROC6.1 (p1 & p2)	JAMSTEC	3	3	3	ZM	S. Watanabe (wnabe@jamstec.go.jp)
MRI-ESM2.0	MRI	3	3	3	ZM	H. Naoe (hnaoe@mri-jma.go.jp) K. Yoshida (kyoshida@mri-jma.go.jp)

parameterization scheme used, its tuning (i.e., adjustment of the scheme's free parameters), as well as other aspects of the simulated climate such as mean wind biases near the tropical tropopause.

The dissipation of resolved waves in the tropical stratosphere, which forces the dynamical QBO, is well known to be sensitive to vertical resolution in the lower tropical stratosphere (Anstey et al., 2016; Geller et al., 2016; Garfinkel et al., 2022; Simpson et al., 2025; Yu et al., 2025). Table 3 indicates the number of levels and upper boundary for each model, as well as their approximate vertical resolutions near the 50 hPa level ($\approx$ 21 km altitude). Vertical profiles of the models' approximate log-pressure layer spacings are shown in Figure 2. Most models have vertical resolution less than 1 km in the lowermost tropi-

https://doi.org/10.5194/egusphere-2026-1165
Preprint. Discussion started: 6 May 2026

Table 3. Model horizontal and vertical resolutions, and primary reference(s). Horizontal resolution in degrees (°) is denoted as longitude × latitude.

Model	Horizontal resolution	Number of vertical levels	Model lid (hPa)	50 hPa Δz (km)	Model reference(s)
BCC-CSM2-MR	T106	46	1.459	0.88	Wu et al. (2019); Lu et al. (2020)
CAS-ESM	1.4° × 1.4°	69	0.01	0.55	Zhang et al. (2020); Chai et al. (2021)
CESM2	1.25° × 0.9°	83	0.008	0.50	Danabasoglu et al. (2020)
E3SMv2	ne30 (≈ 110 km)	72	0.1	1.08	Golaz et al. (2022)
EC-Earth3	TL255	91	0.01	0.68	Döscher et al. (2022); Serva et al. (2024)
ESM4	C96 (≈ 100 km)	50	0.01	1.72	Horowitz et al. (2020)
GRIMs 4.0	T62	91	0.01	0.70	Koo et al. (2023)
HadGEM3GA7.1	0.83° × 0.55°	85	0.01	0.76	Walters et al. (2019)
LMDz6	2.5° × 1.25°	79	0.01	1.07	Hourdin et al. (2020)
MIROC6.1 (p1 & p2)	T85	90	0.004	0.54	Tatebe et al. (2019)
MRI-ESM2.0	TL59	80	0.01	0.63	Yukimoto et al. (2019)

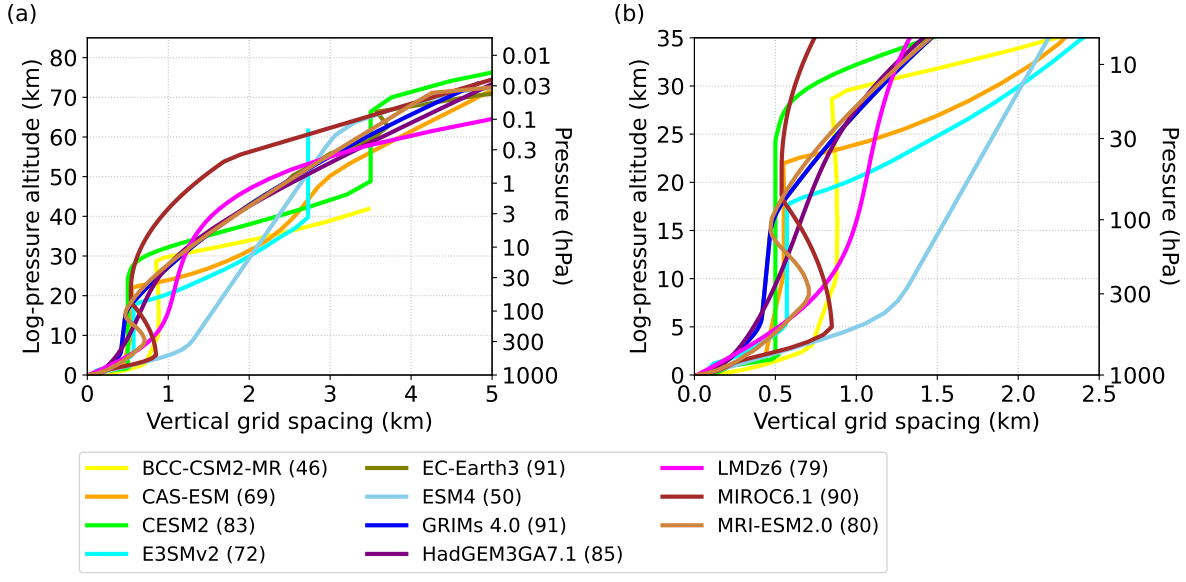

Figure 2. (a) Vertical grid spacings, Δz (km), for models listed in Table 2. (b) As (a), but zoomed in to show Δz in the lower tropical stratosphere. Both p1 & p2 variants of MIROC6.1 have the same vertical grid. The GRIMs 4.0 and EC-Earth3 overlap substantially at altitudes below ≈ 50 km.

cal stratosphere, between 100 hPa and 30 hPa, with the highest-resolution models having grid spacing ≈ 0.5 km near 50 hPa. Sensitivity of QBO simulations to vertical resolution is not well quantified, but it is likely associated with the theoretical pre-

https://doi.org/10.5194/egusphere-2026-1165
Preprint. Discussion started: 6 May 2026

diction that vertical wavelengths of upward propagating equatorial waves decrease as the waves' zonal phase speed approaches the local QBO (i.e., background) zonal wind speed, enhancing the radiative damping of waves or causing them to break and thereby depositing the momentum that drives the QBO. Simulations of the QBO are also sensitive to many other aspects of model formulation (Garfinkel et al., 2022), including horizontal and vertical diffusions and the choice of dynamical core (Yao and Jablonowski, 2015).

Table 4. Non-orographic gravity wave drag and convection parameterizations. AD99: Alexander and Dunkerton (1999), B14: Bechtold et al. (2014), B04: Beres et al. (2004), B15: Bushell et al. (2015), CL15: de la Cámara and Lott (2015), CM02: Charron and Manzini (2002), CS10: Chikira and Sugiyama (2010), E01: Emori et al. (2001) modification of Arakawa and Schubert (1974), H20: Han et al. (2020), H97: Hines (1997), L17 : Larson (2017), L81: Lindzen (1981), LG13: Lott and Guez (2013), O10: Orr et al. (2010), PB09: Park and Bretherton (2009), R13: Rio et al. (2013), S02: Scaife et al. (2002), W19: Wu et al. (2019), Wa: Walters et al. (2019) Y15: Yoshimura et al. (2015), ZM95: Zhang and McFarlane (1995), Z18: Zhao et al. (2018).

Model	Non-orographic GWD scheme	Non-orographic GWD source	Convection scheme
BCC-CSM2-MR	B04	B04	W19
CAS-ESM	B04, CM02	B04, CM02	ZM95, PB09
CESM2	L81	B04, CM02	ZM95, L17
E3SMv2	B04, CM02	B04, CM02	ZM95, L17
EC-Earth3	O10	fixed	B14
ESM4	AD99	fixed	Z18
GRIMs 4.0	none	-	H20
HadGEM3GA7.1	S02	B15	Wa19
LMDz6	LG13	LG13, CL15	R13
MIROC6.1, p1	H97	fixed	CS10
MIROC6.1, p2	H97	fixed	E01
MRI-ESM2.0	H97	fixed	Y15

Other key forcings that potentially affect the simulated QBOs or their teleconnections include ozone, volcanic aerosol, and the 11-year solar cycle. Most models that performed the phase-2 nudging experiments used prescribed ozone forcing, i.e., the simulated winds and temperatures do not affect the ozone distribution. Three models used interactive (i.e., prognostic) ozone: E3SMv2 (linearized), ESM4 and MRI-ESM2 (full chemistry). A QBO in ozone is primarily due to advection by the mean-meridional circulation at lower altitudes of the QBO, and the photochemical ozone response to QBO-induced temperature perturbations at higher altitudes (Butchart et al., 2003; Tian et al., 2006; Zhang et al., 2021). Anomalous heating rates associated with the ozone QBO may in turn influence the dynamical QBO (Shibata and Deushi, 2005; Shibata, 2021), but this feedback is neglected in models that prescribe ozone (i.e., in all but three of the models used here). The potential importance of this feedback is the focus of new QUasi-biennial oscillation and Ozone Chemistry interactions in the Atmosphere (QUOCA) multi-model experiments using chemistry-climate models (Orbe et al., 2025). Time-evolving volcanic aerosol is prescribed in most

https://doi.org/10.5194/egusphere-2026-1165
Preprint. Discussion started: 6 May 2026

QBOi phase-2 models, though two models omit it (GRIMs 4.0 and LMDz6). Likewise, almost all models prescribe an 11-year solar cycle in their radiative forcing (LMDz6 is the sole exception). The solar cycle is not expected to have a significant direct impact on the simulated QBOs (Hamilton, 2002) but could potentially result in interference with the QBO's modulation of polar vortex variability (e.g., Matthes et al., 2010) or its modulation of the MJO (e.g., Hood et al., 2023).

4.2 Evaluation of nudging in phase 2 models

In this section basic aspects of the phase 2 model simulations are evaluated to assess that the nudging is performing as intended in the tropical stratosphere, i.e., reducing or removing QBO biases in **Exp1-ObsQBO** and eliminating tropical stratospheric variability in **Exp1-NoQBO**. The extent to which the tropically confined nudging has any systematic impact on the extra-tropical stratospheric climate during winter or the amount of polar vortex variability is also assessed. A more detailed investigation of QBO-teleconnections in the phase-2 experiments is presented in Andrews et al. (2026).

Figure 3 shows the evolution of monthly zonal-mean zonal wind in the tropical stratosphere in **Exp1** (left column) and **Exp1-ObsQBO** (right column) for the last 20 years of the simulations, and for the 100–5 hPa altitude range where the QBO in **Exp1-ObsQBO** is nudged (Figure 1a). The zonal-mean zonal wind from the ERA5 reanalysis, which is the target state for the nudging, is shown in the left column opposite the GRIMs **Exp1-ObsQBO** panel (the GRIMs model did not perform **Exp1**). For the nudged simulations (**Exp1-ObsQBO**) all the models track the QBO phase evolution seen for ERA5, including the QBO disruptions in early 2016 and early 2020 (Newman et al., 2016; Osprey et al., 2016; Anstey et al., 2021). Between 10 and 70 hPa most models also represent the amplitude of QBO westerly and easterly phases realistically, as expected since the 5-day nudging timescale is short compared to the timescale on which the QBO winds evolve. Discrepancies between models and ERA5 are apparent below 70 and above 10 hPa where the nudging strength tapers off (Figure 1a). Two models, BCC-CSM2-MR and CAS-ESM, resemble the ERA5 QBO less closely than the other models, especially at higher altitudes in CAS-ESM where a strong westerly bias is present, but the overall phase evolution is nevertheless synchronized with that of the observed QBO.

The free-running simulations (**Exp1**, Figure 3, left column) show a range of periods, amplitudes and vertical extents of simulated QBO-like variability. Westerly and easterly zonal wind regimes descending through the tropical stratosphere, with periods longer than a year and distinct from the annual cycle, are seen in all models. Moreover, for several of the models these zonal-mean zonal wind oscillations closely resemble the ERA5 QBO in their periods, amplitudes, and vertical extents (e.g., MRI-ESM2-0, HadGEM3GA7). Nonetheless the model QBO amplitudes are often weaker than those for ERA5 at the lowest QBO altitudes (50 hPa and below), a known common bias in QBO simulations (Richter et al., 2020; Bushell et al., 2022). Zonal wind variability is less realistic in E3SM-2-0 and ESM4, which used the full-field nudging and also have the coarsest vertical resolution in the 20–30 km layer, with grid spacings of more than 1 km. Large overall westerly biases, with limited downward descent of easterly wind phases are apparent in the CAS-ESM and ESM4 simulations. Broadly, inter model differences in the representation of the QBO in phase-2 **Exp1** are similar to those for phase-1 **Exp1** (Bushell et al., 2022), and therefore not unexpected, though note that not all phase-2 models participated in phase-1, and vice-versa. Comparing the **Exp1**

https://doi.org/10.5194/egusphere-2026-1165
Preprint. Discussion started: 6 May 2026

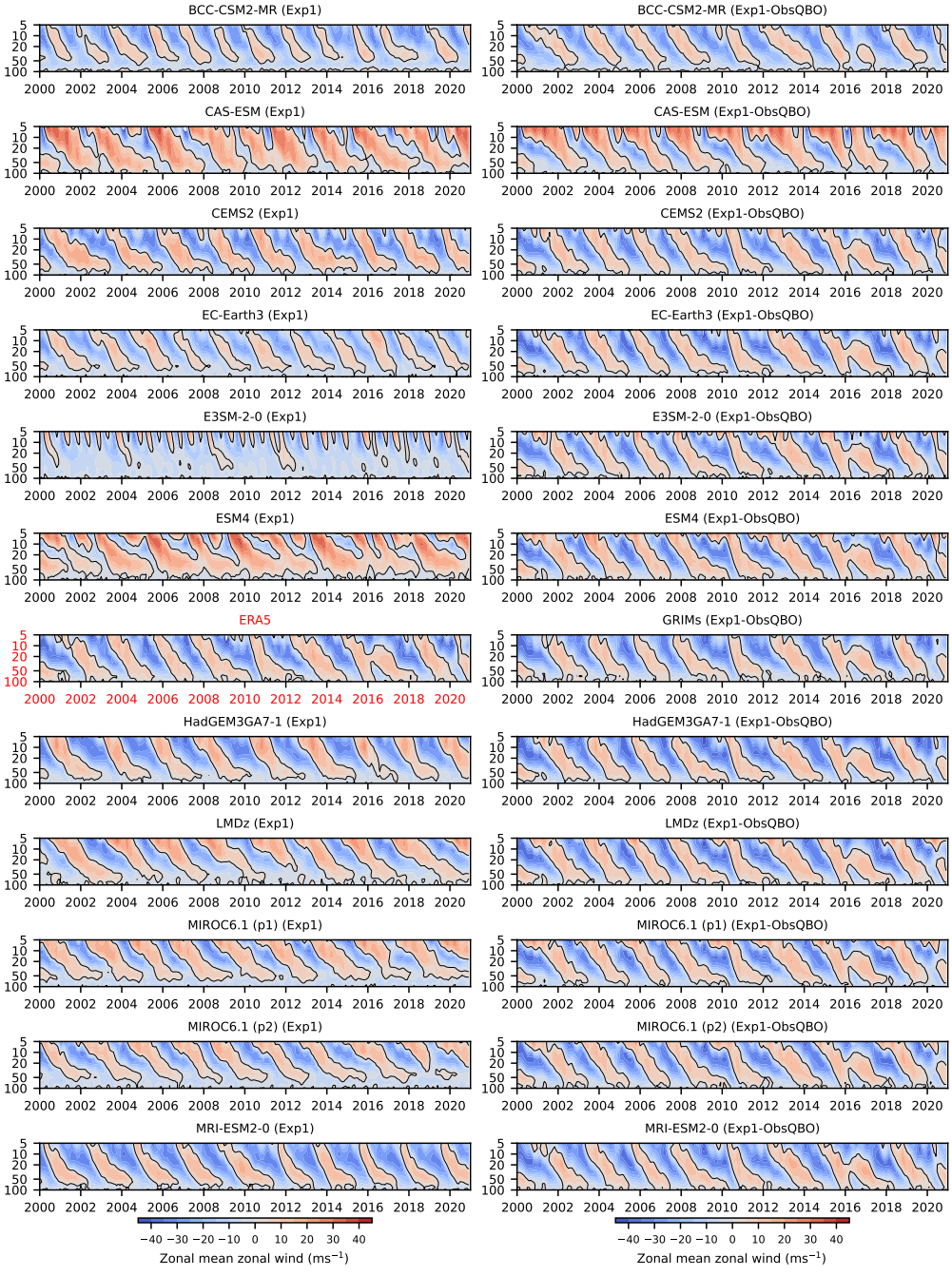

Figure 3. Hovmöller diagrams of the vertical profile (100–5 hPa) of monthly-mean zonal-mean zonal wind, averaged from 5°S to 5°N for 2000–2020 for the participating models for **Exp1** (left) and **Exp1-ObsQBO** (right). GRIMs did not perform **Exp1** and instead corresponding data from ERA5 are shown. When more than one realization was available for a particular experiment and model, results from the realization labeled "r1" in the database are shown.

https://doi.org/10.5194/egusphere-2026-1165
Preprint. Discussion started: 6 May 2026

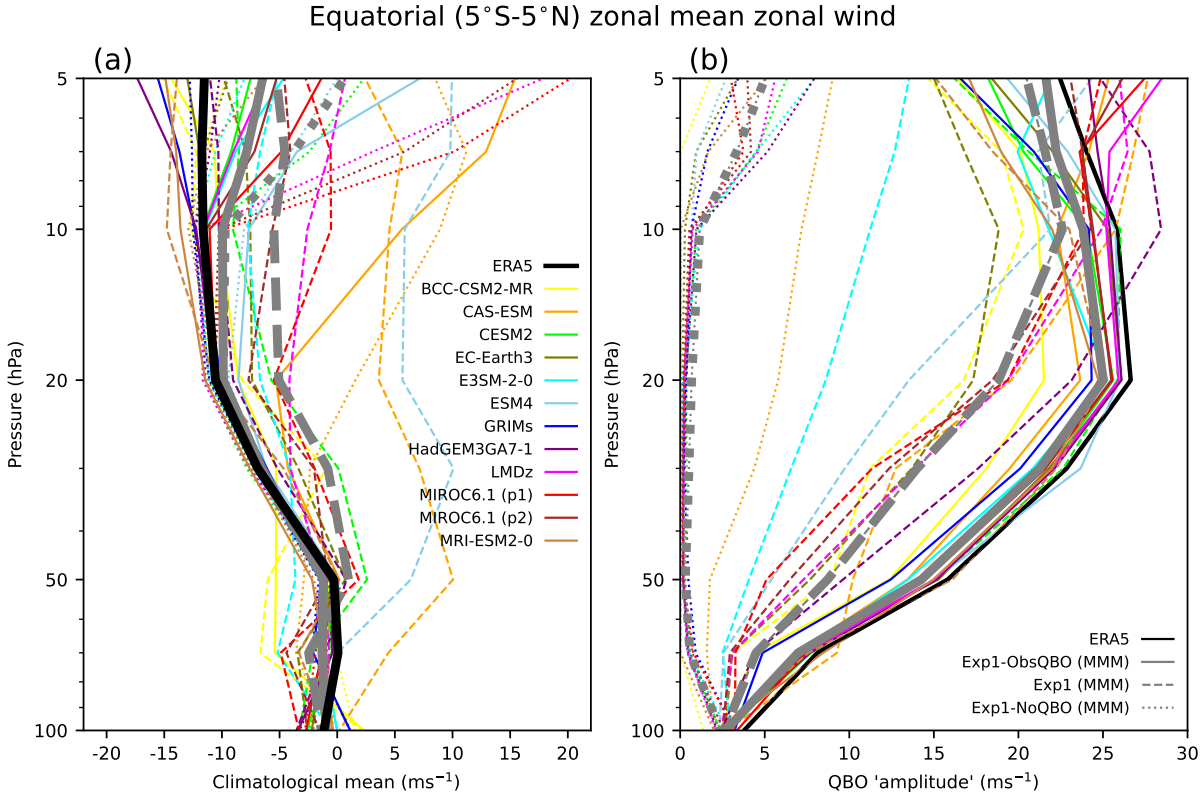

Figure 4. Vertical profiles of the time mean (a) and standard deviation (b) of monthly equatorial (5°S–5°N) zonal-mean zonal winds for 1979–2020 for the participating models (coloured lines) compared to ERA5 (black). **Exp1**, **Exp1-ObsQBO** and **Exp1-NoQBO** are shown by dashed, solid and dotted lines respectively. Thick grey lines denote the multi-model mean. In (b) the standard deviation is calculated after subtracting the mean annual cycle and then multiplied by $\sqrt{2}$, which approximates the mean QBO amplitude when the QBO is the dominant mode of variability in the equatorial stratosphere (Dunkerton and Delisi, 1985).

and **Exp1-ObsQBO** results (left and right columns of Figure 3) confirms that the nudging is generally successful at eliminating QBO biases and inter-model differences in the phase-2 models.

Equatorial (5°S–5°N) vertical profiles of the zonal-mean zonal wind climatology (Figure 4a) for both nudged experiments (**Exp1-ObsQBO, Exp1-NoQBO**) closely follow the corresponding ERA5 climatology in the core nudging region (10–70 hPa), as expected. Between 10 hPa and 5 hPa the nudging strength tapers to zero (Figure 1a) and the model climatologies begin to diverge from ERA5, possibly reflecting biases in the simulated SAO, although it should be noted that reanalysis winds are less well constrained by radiosonde observations in this region (Kawatani et al., 2016). Climatologies of the experiment without nudging (**Exp1**; dashed lines) generally have westerly biases between 50 and 10 hPa with respect to reanalysis, though the westerly biases are much more substantial in CAS-ESM and ESM4 with climatological westerlies replacing the observed climatological easterlies. Overall, these features are consistent with westward wave forcing that is too weak in the models

https://doi.org/10.5194/egusphere-2026-1165
Preprint. Discussion started: 6 May 2026

leading to weak easterly QBO phases, as noted in previous studies using earlier generations of the models (e.g., Stockdale et al., 2022; Holt et al., 2022). Finally, it is notable that **Exp1** shows some inter-model spread in climatological zonal-mean zonal winds in the 70–100 hPa layer, below the region where the QBO dominates the variability of tropical stratospheric winds. Although this spread is small (≈ 5 m/s) compared to inter-model spread at higher altitudes, it is potentially important because waves propagating through this region affect the forcing of QBO phases above. Small changes in selective wave filtering in the lower stratosphere due to subtle changes in the background wind can have large knock-on effects on the evolution of the QBO wind above due to the effects of decreasing atmospheric density with altitude (Anstey et al., 2016; Alexander et al., 2021).

Vertical profiles of the standard deviation of deseasonalized zonal-mean zonal wind, multiplied by $\sqrt{2}$, are shown in Figure 4b. This diagnostic is considered a good approximation to the QBO amplitude under the assumption that the QBO is the dominant component of interannual variability (Dunkerton and Delisi, 1985), as is the case for the nudged QBOs (**Exp1-ObsQBO**) and those models with realistic QBO-like variability in Figure 3 for **Exp1**. When the variability is less realistic (such as in E3SM-2.0) the diagnostic still quantifies the equatorial variability, as it does for **Exp1-NoQBO** and for simplicity is referred to hereinafter as the QBO wind amplitude. In **Exp1** (dashed curves) the models generally underestimate the QBO amplitude compared to ERA5, by up to 50% at 50 hPa for the multi-model mean (thick gray line) although individual model results vary widely. Nudging to the observed QBO (**Exp1-ObsQBO**, solid curves) brings the models' variability into much closer agreement with ERA5, as expected, although in general the models QBO amplitudes remain slightly weaker than the amplitude for the reanalysis. Nonetheless this significant reduction in the amplitude bias supports the decision to nudged only the zonal component of the winds since when both meridional and zonal components of the wind in addition to temperature were nudged in another study, albeit with a shorter relaxation timescale and the nudging operating through the model domain, the QBO bias correction was less successful, at least for the winds (Hardiman et al., 2017). Above the core nudging region (10–70 hPa), variability is stronger than ERA5 in some models and weaker in others. Below the core nudging region, between 70 hPa and the tropical tropopause, models almost uniformly underestimate the zonal-mean zonal wind variability compared to ERA5, by up to 50% for the multi-model mean. It should be noted that since zonal asymmetries are larger close to the tropopause than above (e.g., due to the Walker Circulation) the zonal-mean diagnostic used here may be insufficient at these altitudes to properly assess the potential impacts of wind biases in this region on upward wave propagation. Variability of the zonal-mean zonal wind in the experiment nudged to the ERA5 climatology (**Exp1-NoQBO**, dotted curve) is almost entirely suppressed in the 10–70 hPa region in almost all models, as intended.

Latitudinal profiles of the QBO wind amplitude at 50 hPa are shown in Figure 5. The 50 hPa level is chosen because the equatorial QBO amplitude at that level is substantially underestimated by phase-2 models (Figure 4) and models in general (e.g., Richter et al., 2020). In addition the 50 hPa level is often used as a QBO index when analysing QBO teleconnections (e.g., Anstey and Shepherd, 2014; Son et al., 2017; Martin et al., 2021). The underestimated equatorial QBO amplitude at 50 hPa in **Exp1** is associated with a substantial latitudinal narrowing of the simulated QBOs in comparison to ERA5 (Figure 5a, dashed curves), consistent with QBO amplitude decaying with distance from the equator. Narrower QBOs could potentially lead to weaker teleconnections to higher latitudes (Hansen et al., 2013). The nudging profile (Figure 1b) used in **Exp1-ObsQBO** strengthens the QBO wind amplitude across the tropical band (Figure 5a, solid curves), bringing the width of the simulated

https://doi.org/10.5194/egusphere-2026-1165
Preprint. Discussion started: 6 May 2026

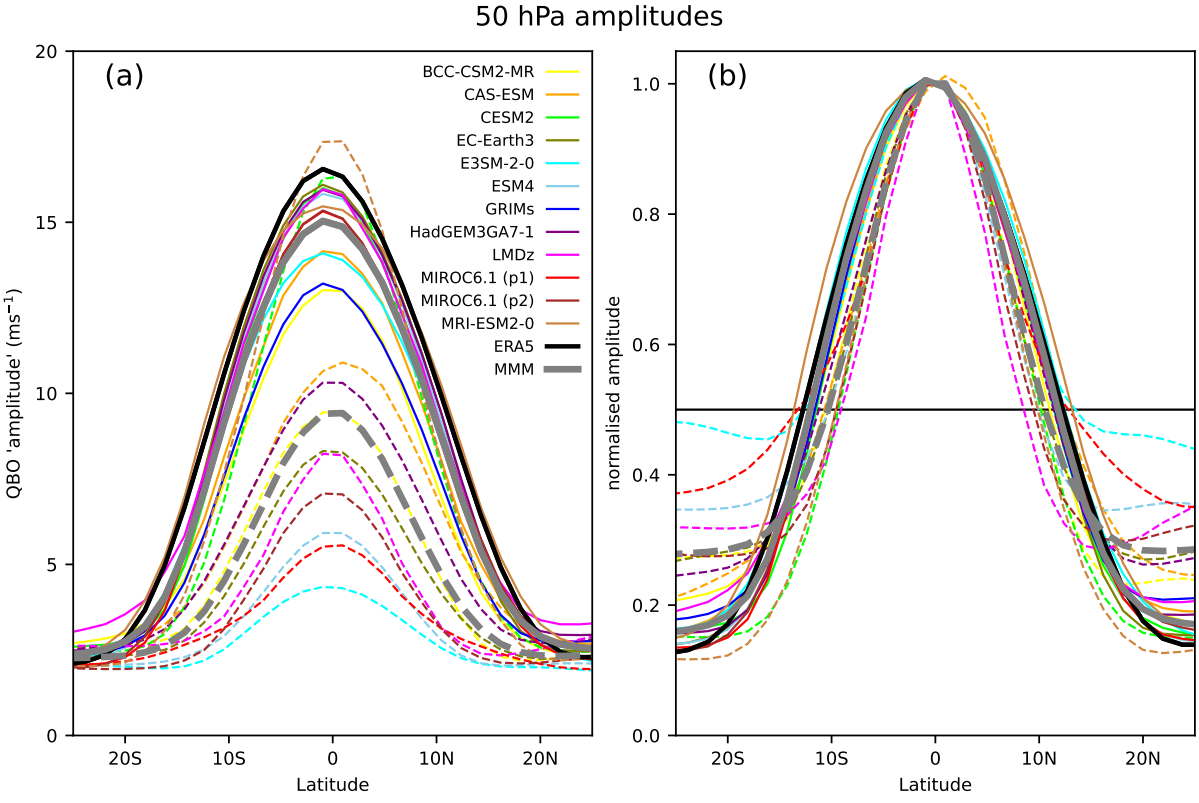

Figure 5. (a) QBO wind amplitude defined as in Figure 4b, but for latitudinal profiles at 50 hPa. Only **Exp1** (no nudging; dashed) and **Exp1-ObsQBO** (nudging to the observed QBO; solid) are shown. (b) As (a), but with each profile normalized by its peak value. The horizontal black line denotes the half-amplitude (50% of peak value), which is partially used in determining the optimum width for the nudging (see Section 2)

QBO into close agreement with ERA5, albeit still slightly less. The normalized amplitudes in Figure 5b confirm that the apparent narrower simulated QBOs in Figure 5a compared to ERA5 are not simply artifacts of the peak amplitudes at the equator being too weak. On average, at half maximum amplitude (horizontal line in Figure 5b), the simulated QBOs in **Exp1** (dashed grey line) are $4.2° \pm 1.7°$ (17%) narrower than the ERA5 QBO (black line), improving to just $1.2° \pm 0.7°$ (5%) narrower in **Exp1-ObsQBO** (solid grey line).

As well as bias correcting the QBO amplitudes in **Exp1-ObsQBO** another important consequence of the nudging is the synchronization of the cycle-to-cycle variations in the QBO amplitude and phase with ERA5 and between the individual ensemble members (Figure 6). In reality, cycle-to-cycle variations in QBO amplitude and phase are part of the natural internal variability of the atmosphere and the nudging in **Exp1-ObsQBO** creates an artificial situation of an ensemble with a near "perfectly predictable" QBO in the ensemble mean. This multi-year predictable QBO signal does not result from initial conditions and, instead, is essentially externally forced (i.e., by the nudging). Hence, the ensemble of **Exp1-ObsQBO** simulations can

https://doi.org/10.5194/egusphere-2026-1165
Preprint. Discussion started: 6 May 2026

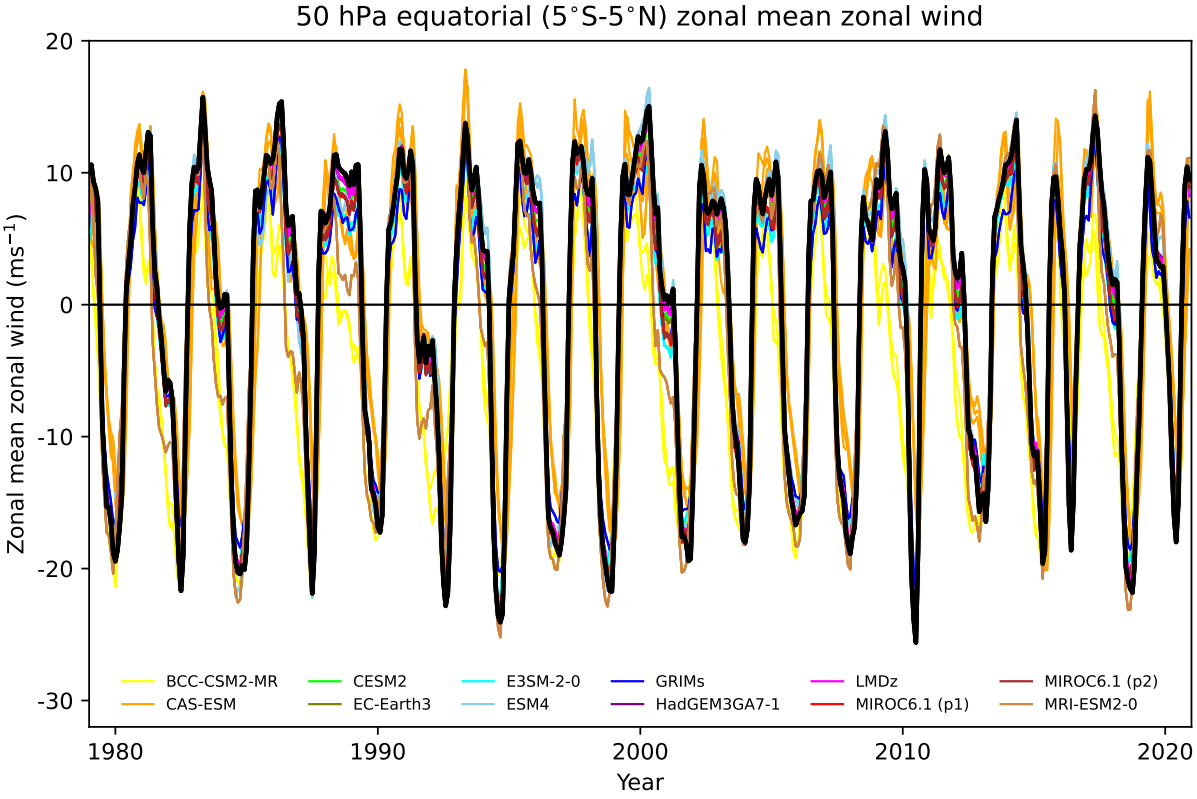

Figure 6. Time series of monthly-mean, zonal-mean zonal wind at 50 hPa and averaged from 5°S to 5°N for 1979–2020 for ERA5 (black curve) and for the individual **Exp1-ObsQBO** simulations (coloured curves). For each model each ensemble member is shown as a separate line.

be utilized to assess the remote response (i.e., teleconnections) of the nudged QBO signal in the same way that the response to prescribed SSTs has previously been assessed (e.g., Rodwell et al., 1999). Further development of this application of the nudging can be found in Andrews et al. (2026).

To assess the impact that QBO biases have on its teleconnections to the extratropics it is important that the QBO bias correction or nudging used in the phase 2 experiments does not inadvertently lead to systematic changes to a model's climatology outside the tropics where the nudging is applied (Figure 1b). The climatological stratospheric polar-night jets for the nudged experiments are shown by the contours in Figure 7. For the NH, December-January-February (DJF) is shown, while for the SH, September-October-November (SON) is shown as these are the seasons in which the teleconnections between the QBO and polar vortex are generally most prominent (e.g., Butchart, 2022). Corresponding ERA5 climatologies are shown in Figure 8a,b though the aim here is not to evaluate in detail the climatologies of the individual models. Instead, the reader is referred to individual model evaluation papers (see Table 2 for references). Nonetheless all the models broadly reproduce for **Exp1** the reanalysis climatology, but with some showing large biases in the strength of the jet or in the tilt of the jet axis (not shown

https://doi.org/10.5194/egusphere-2026-1165
Preprint. Discussion started: 6 May 2026

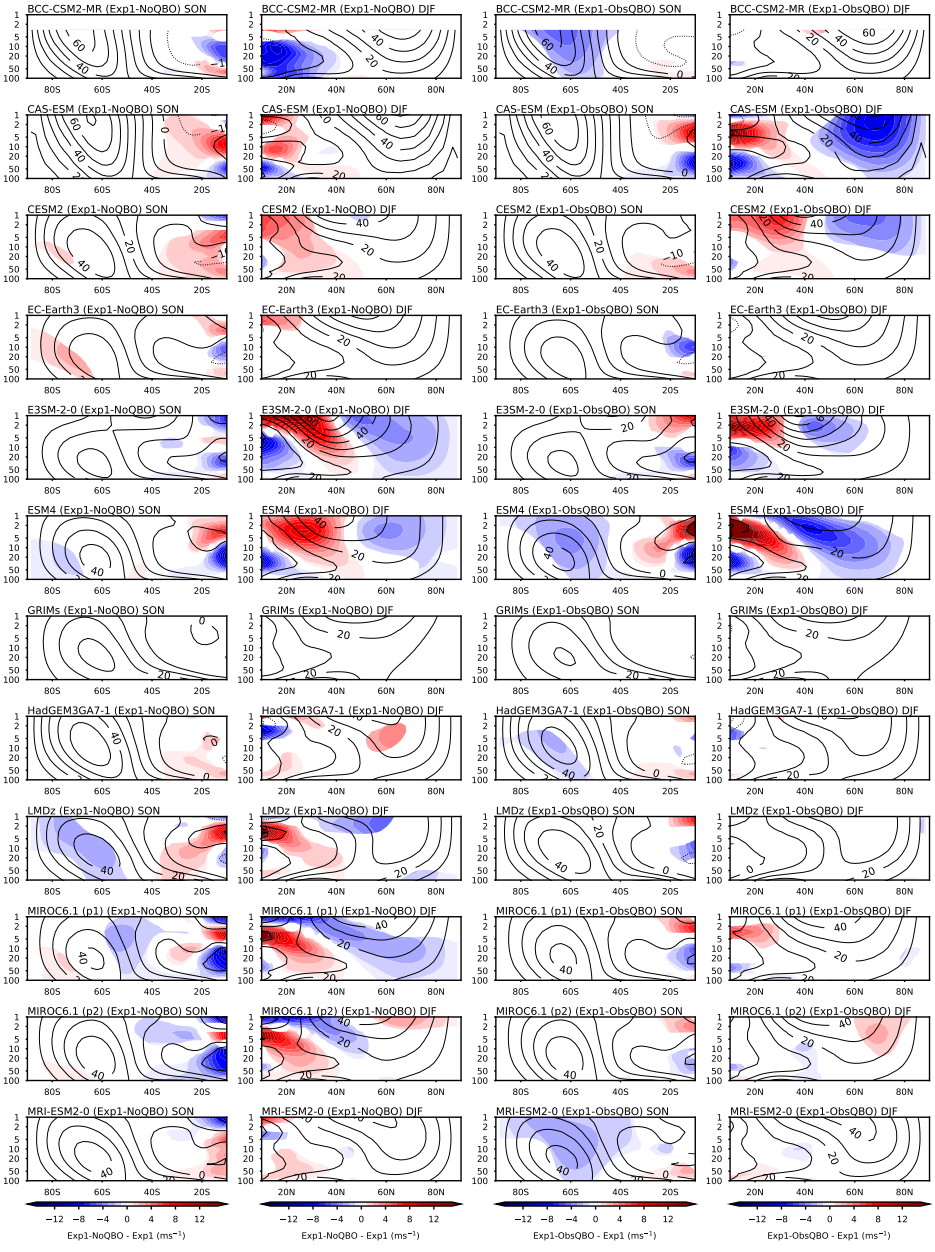

Figure 7. For the nudged simulations **Exp1-NoQBO** (left, 2 columns) and **Exp1-ObsQBO** (right 2 columns) climatological stratospheric polar night jets (contours) for December-January-February (DJF) in the Northern, and September-October-November (SON) in the Southern Hemispheres. The 1979–2020 mean of the seasonal and zonal-mean zonal wind (ms^{-1}) are shown, using all available realizations for each model. Coloured shading indicates the differences between the nudged and corresponding free-running simulations i.e., **Exp1-NoOBO** minus **Exp1** (left 2 columns) and **Exp1-ObsQBO** minus **Exp1** (right 2 panels). Shading is only shown where the differences are statistically significant at the 95% level by a 2-sided t-test, and its contour interval is 1 ms^{-1}. The region 10°S–10°N is not shown to exclude differences resulting directly from the tropical nudging. Differences are not shown for GRIMs as **Exp1** data was unavailable.

https://doi.org/10.5194/egusphere-2026-1165
Preprint. Discussion started: 6 May 2026

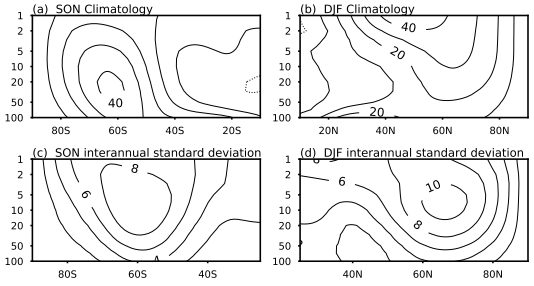

Figure 8. ERA5 climatological stratospheric polar night jets for (a) SON in the Southern and (b) DJF in the Northern Hemisphere. The 1979–2020 mean of the seasonal and zonal-mean zonal wind (ms^{-1}) are shown. (c) and (d) Interannual standard deviation (ms^{-1}) of the SON and DJF seasonal means, for the Southern and Northern Hemisphere, respectively.

but see Figure 7 for the nudged simulations). Despite the varied model biases, the shading in Figure 7 shows that in most models the differences between the nudged simulations (**Exp1-ObsQBO** and **Exp1-NoQBO**) and **Exp1** from the same model are generally small, with many differences being ≈ 5 ms^{-1} or less against background values in the 30–60 ms^{-1} range. Where there are differences in the northern middle and high latitudes the jets are typically weaker in the nudged simulations compared to **Exp1** which is consistent with westerly biased equatorial climatological winds between 50 and 10 hPa in **Exp1** (Figure 4a), assuming a similar process to the observed NH vortex response to the QBO (i.e., equatorial easterlies weaken the vortex and equatorial westerlies strengthen it). Any differences in the SH middle and high latitudes are generally smaller than in the NH and are not consistent in sign between models. In both hemispheres the differences from **Exp1** tend to be larger in the subtropics than at higher latitudes. In those cases where a high-latitude difference is evident, the low-latitude response tends to have opposite sign, consistent with a shift in the jet latitude. Subtropical differences are generally larger relative to the background flow than those at higher latitudes, and may result from changes in the QBO-induced mean-meridional circulation as well as the response of equatorward-propagating planetary waves responding to the effects of the nudging, especially when full field nudging is used (e.g., E3SM-2-0 and ESM4). Overall, Figure 7 indicates that the climatological polar-night jet wind structure is very similar in all three experiments (**Exp1**, **Exp1-ObsQBO**, and **Exp1-NoQBO**).

As with the climatology the phase-2 models broadly capture the interannual variability of SH SON and NH DJF seasonally averaged zonal-mean zonal winds seen in Figure 8c,d for ERA5. The corresponding model results for the nudged simulations (**Exp1-NoQBO** and **Exp1-ObsQBO**) are shown by the contours in Figure 9. There is a wide inter-model spread in the overall strength and spatial distribution of the interannual variability. In all models, differences between the nudged simulations and **Exp1** (coloured shading in Figure 9) are generally small (between -1 and 1 ms^{-1}). In general the responses are not large in comparison to the background strength of the variability, and no consistent response is seen across the multi-model ensemble. Some models show a slightly larger response (e.g., BCC-CESM2, CESM2, LMDz) and, interestingly, they tend to have a similar response in both of the nudged experiments, which as noted previously have more easterly climatological tropical winds than **Exp1** (Figure 4a). Overall however, the interannual variability in SH SON and NH DJF in these models has little

https://doi.org/10.5194/egusphere-2026-1165
Preprint. Discussion started: 6 May 2026

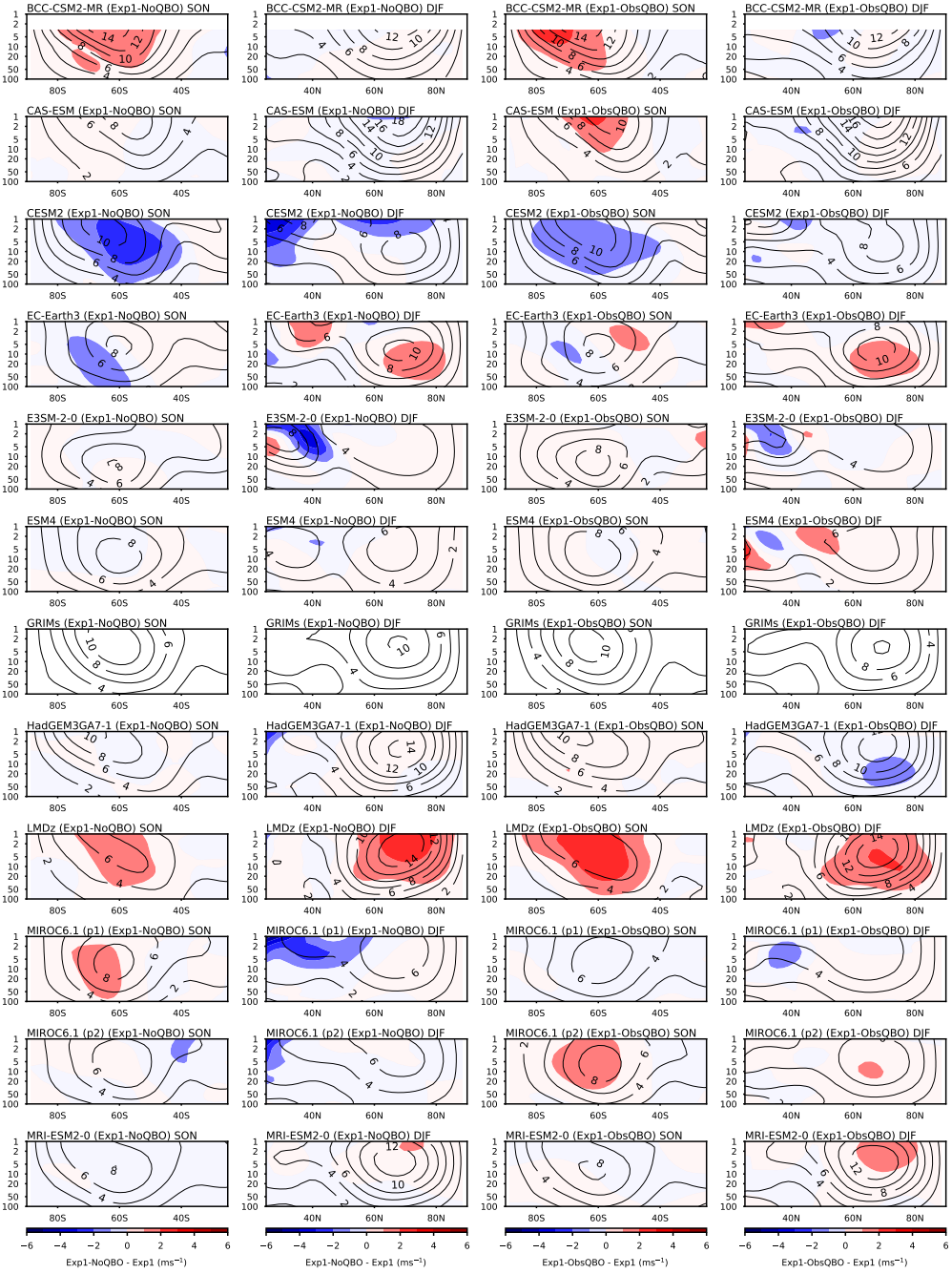

Figure 9. As Figure 7, but for the interannual variability of the polar-night jet. Contours (ms^{-1}) show the interannual standard deviation of the zonal-mean zonal wind seasonal means whose climatology (i.e., 1979–2020 mean) is shown in Figure 7. Coloured shading shows differences of the nudged runs from the corresponding interannual variability in the simulations without nudging (left 2 columns: Exp1-NoOBO minus **Exp1**, right 2 columns: **Exp1-ObsQBO** minus **Exp1**). The plots do not show the tropics (20°S–20°N) where the direct impact of the nudging dominates the interannual variability (i.e., the QBO). Note that for **Exp1** data is not available for the GRIMs hence differences are not shown for that model.

https://doi.org/10.5194/egusphere-2026-1165
Preprint. Discussion started: 6 May 2026

sensitivity to the imposition of nudging, and consequently interannual variability in the two nudged experiments is very similar. Therefore, the large contrast in tropical stratospheric variability between **Exp1-ObsQBO** (realistic QBO winds) **Exp1-NoQBO** (completely suppressed) does not contribute significantly to the extent to which the polar night jet varies from year to year. However this does not imply that high-latitude variability cannot be modulated by the tropics if the QBO acts to "organize" the variability (as evidenced by the observed Holton-Tan correlation) without appreciably changing the overall strength of the variability.

5 Concluding remarks

A protocol for coordinated experiments in which the tropical stratosphere is nudged toward reanalysis has been used for phase-2 of the APARC QBOi activity. The experiments test the impact of bias correcting the QBO on other aspects of simulated climate, such as extratropical teleconnections or tropical wave driving of the QBO. The two experiments adapt the well-known AMIP experiment by adding nudging in the tropical stratosphere, so that the atmospheric circulation "sees" either the observed evolution of the QBO over the recent historical record (1979–2020; **Exp1-ObsQBO**) or completely suppressed tropical stratospheric variability (**Exp1-NoQBO**).

Validation of initial results from the experiments by 12 participating models demonstrates that the nudging substantially corrects QBO biases as intended. In 9 models the nudging has been implemented on the zonal-mean component of the zonal wind, allowing tropical waves in the models to propagate through a realistic background state over the 70–10 hPa region of the lower tropical stratosphere. The other models implemented full-field nudging, but the 5-day nudging timescale allows some freedom for short-period waves to evolve unconstrained by the nudging. In the extratropics, the models show weak or no systematic impact of the tropical nudging on the climatological polar night jets or their interannual variability in either hemisphere during the most dynamically active seasons (SON in the SH, DJF in the NH). This suggests the climatology and strength of variability of the polar-night jet are insensitive to model errors in tropical stratospheric variability. However this is separate from the question of whether QBO teleconnections may be a source of predictive skill and the extent to which reduction of QBO biases can improve model representation of these teleconnections. A useful feature of **Exp1-ObsQBO** is that nudging to reanalysis implies that QBOs are synchronized across the models, just as SSTs are synchronized due to the AMIP boundary conditions, and an ensemble-mean teleconnections signal can be diagnosed. A thorough analysis of the response of extratropical teleconnections to the QBO bias correction in the phase-2 nudged runs is given by Andrews et al. (2026).

The experiments described here provide a useful baseline for further extensions of the nudging method to explore the origin and consequences of QBO biases. Using nudging the impact of changing model parameters (e.g., non-orographic gravity wave drag parameter settings) on QBO wave forcing can be investigated without these changes affecting the background QBO winds and their impact on QBO predictability examined by switching off the nudging at a chosen "initialization" time. For teleconnections, varying the nudging profile can be used to adjust the downward extent or width of the QBO winds to test sensitivities and causality; similar experiments using idealized tropical winds have been widely reported in the literature (Hansen et al., 2013; Anstey and Shepherd, 2014; Matthes et al., 2010). Repeating the current QBOi phase-2 experiments but

https://doi.org/10.5194/egusphere-2026-1165
Preprint. Discussion started: 6 May 2026

with annual repeating SSTs instead of observed SSTs would allow the effects of QBO teleconnections and SST teleconnections on the variability of the stratospheric polar vortex or the tropical troposphere to be separated and the additivity of the responses assessed. To assess the impact of bias-corrected QBOs on the initialized simulations the nudging technique and profiles used here could also be applied to seasonal hindcasts. Novel features of the present experiments that are desirable in any further experiments are the use of a multi-model approach to assess robustness, and use of reanalysis as the target state to make the simulations directly comparable with observations.

Data availability. Model output for the QBOi experiments described in this paper are kindly hosted by the NERC Centre for Environmental Data Analysis (CEDA), UK. Access can be requested by contacting the QBOi coordinators (https://aparc-climate.org/activities/qboi/) and applying via the JASMIN online portal[2], as described at https://doi.org/10.5281/zenodo.19059510. ERA5 data was obtained from the Copernicus Climate Change Service (C3S) Climate Data Store (CDS) (Hersbach et al., 2023).

Appendix A: Nudging methodology

"Nudging" refers to imposing a relaxation term in a model's prognostic equations that forces the model toward a target state. In both nudging experiments, **Exp1-ObsQBO** and **Exp1-NoQBO**, only the zonal-mean component of the zonal wind is nudged (unless models perform the full-field variant described in Sec. A3). The nudging is equivalent to a forcing in the zonal momentum equation of the form $-\alpha(\overline{u} - \overline{u_r})$, where $\overline{u}$ is the model's zonal-mean zonal wind, $\overline{u_r}$ is the target state for the relaxation, and $\alpha = 1/\tau$ is the spatially varying relaxation rate, with τ being the nudging timescale. The spatial variation of α is described in Section A1. The different target states for **Exp1-ObsQBO** and **Exp1-NoQBO** are described in Section A2.

A1 Vertical and latitudinal profiles

At maximum strength the nudging timescale is $\tau = 5$ days, which is expected to be sufficient to constrain the slowly evolving QBO winds. The altitude profile of the nudging (Figure 1a) is given by

$$\frac{1}{4}\left[1 - \tanh\left(\frac{p - p_b}{\Delta p_b}\right)\right]\left[1 + \tanh\left(\frac{p - p_t}{\Delta p_t}\right)\right] \tag{A1}$$

where

$$p_b = 80 \text{ hPa},\ \Delta p_b = 5 \text{ hPa},\ p_t = 8 \text{ hPa},\ \Delta p_t = 0.5 \text{ hPa}$$

specify the bottom (p_b) and top (p_t) pressure altitudes of the nudging region, and the parameters Δp_t and Δp_b control the width of the transition between nudged and free (i.e., non-nudged) regions. The nudging rate at a given latitude should be constant on model levels. The pressure-levels profile (A1) should be converted to model levels using typical pressures on those levels.

[2]https://help.jasmin.ac.uk/docs/short-term-project-storage/apply-for-access-to-a-gws/

https://doi.org/10.5194/egusphere-2026-1165
Preprint. Discussion started: 6 May 2026

The latitude profile of the nudging (Figure 1b) is given by

$$\frac{1}{4}\left[1-\tanh\left(\frac{\phi-\phi_N}{\Delta\phi}\right)\right]\left[1+\tanh\left(\frac{\phi-\phi_S}{\Delta\phi}\right)\right] \tag{A2}$$

where

$$\phi_N = 12^\circ,\ \phi_S = -12^\circ,\ \Delta\phi = 2^\circ$$

specify the Northern Hemisphere (ϕ_N) and Southern Hemisphere (ϕ_S) latitudinal boundaries of the nudging region, and $\Delta\phi$ controls the width of the transition between nudged and non-nudged regions. The full spatial variation of the nudging relaxation rate α is obtained by multiplying the maximum rate, $1/(5\ \text{days})$, by the profiles (A1) and (A2). This should constrain a model's zonal-mean zonal wind to follow the prescribed target state ($\overline{u_r}$) in the indicated region of the tropical stratosphere (Figure 1) while allowing free evolution of zonal asymmetries (waves) in the nudged region, and free evolution of the full 3D circulation everywhere else.

A2 Target states

Exp1-ObsQBO and **Exp1-NoQBO** use the same spatial variation of nudging relaxation rate (α), but differ in their target states ($\overline{u_r}$). In **Exp1-ObsQBO**, the target state used to represent the observed QBO is the zonal-mean zonal wind from the ERA5 reanalysis (Hersbach et al., 2020). ERA5 is a state-of-the-art modern reanalysis covering the 1940–present period that assimilates a range of observational types including, crucially for the QBO, wind observations from near-equatorial radiosondes. In comparison to the long-running record (1953–present) of near-equatorial radiosonde wind observations compiled by the Freie Universität Berlin (Naujokat, 1986), modern reanalysis products generally represent the QBO well (Fujiwara et al., 2022, Chapter 9). At the equator there are large gaps in the radiosonde observing network over the tropical oceans, and reanalysis winds are correspondingly more uncertain at these longitudes (Kawatani et al., 2016). However as these uncertainties are smaller than biases typically seen in QBO wind amplitudes in the phase-2 models (Figure 4), ERA5 zonal-mean zonal wind is believed to provide a sufficiently accurate representation of the observed QBO.

Use of a common reanalysis avoids the choice of target state being a potential source of inter-model differences. While ERA5 is recommended, modellers may use a different reanalysis if this is required in order to perform the experiments with reasonable efforts (for example, if the model is already set up to nudge toward a different reanalysis and the effort to switch to ERA5 would be prohibitive). Some known differences between reanalyses that should be considered if an alternative reanlaysis is used are:

- During the 2000-2006 period ERA5 exhibits temperature biases that were corrected in a re-run of this period, ERA5.1, as described in an ECMWF technical report[3]. ERA5.1 shows slightly larger QBO amplitude than ERA5 in the 2000–2006 period. However, tropical wind differences between the two are small (e.g., Figure 25 of the above report) and unlikely to have a significant impact on the QBOi nudging experiment results. Modellers may choose to substitute ERA5.1 for ERA5 during the 2000–2006 period, but this is not considered essential.

[3]https://www.ecmwf.int/en/elibrary/19362-global-stratospheric-temperature-bias-and-other-stratospheric-aspects-era5-and

https://doi.org/10.5194/egusphere-2026-1165
Preprint. Discussion started: 6 May 2026

- MERRA-2 generally represents the QBO well due in part to its inclusion of parameterized non-orographic gravity wave drag that is tuned to improve the QBO (Coy et al., 2016). Early in its record there are unrealistic tropical winds near 10 hPa (Kawatani et al., 2016). MERRA-2 begins in 1980.
- NCEP-CFSR is less suitable than other modern reanalyses since its QBO has some unrealistic features in the period before 1990 (Fujiwara et al., 2022, Chapter 9).
- The older NCEP reanalyses, NCEP-NCAR (R1) and NCEP-DOE (R2), should be avoided due to their substantially weaker QBO amplitudes, as compared to other reanalyses and to radiosonde winds (Fujiwara et al., 2022, Chapter 9).

A3 Full-field experiment variant

Nudging only the zonal-mean flow component is infeasible in some AGCMS, depending on the details of model formulation (for example, the type of dynamical core). A full-field variant of the experiments allows such models to participate in the experimental protocol. Here "full-field" refers to nudging the full 3D flow, i.e., both zonal-mean and zonally asymmetric flow components. The following full-field experiment names are designated:

Exp1-ObsQBO-full: As Exp1-ObsQBO but using full-field nudging. Since the nudging is confined to the tropics, it is expected that full-field nudging is suitable for studying QBO teleconnections. For studying the forcing (wave driving) of the QBO, full-field nudging allows study of parametrized waves, as well as resolved waves whose timescales are short compared to the nudging timescale (5 days).

Exp1-NoQBO-full: As Exp1-NoQBO but using full-field nudging. Since the climatological target state will be mostly zonally symmetric, waves in the tropical stratosphere should be mostly damped out by the nudging unless their timescales are short compared to the 5-day nudging timescale.

A4 Comparison with SNAPSI

The SNAPSI project (Hitchcock et al., 2022) specifies coordinated experiments in which the zonal-mean stratospheric circulation is nudged toward reanalysis in order to study the tropospheric impacts of sudden stratospheric warming (SSW) events using a multi-model ensemble. For reference, and for the benefit of modellers considering performing both SNAPSI and QBO experiments, we summarize here their similarities and differences. In SNAPSI and QBOi, the following aspects are *the same*:

- Only the zonal-mean component of the flow is nudged.
- There is no nudging in the troposphere (from the surface up to $\sim$ 100 hPa).

Compared to the SNAPSI experiments, the following aspects are *different in QBOi*:

- Only the zonal wind is nudged (SNAPSI also nudges the temperature).
- Nudging is zero outside the tropics (SNAPSI nudges equally at all latitudes).

https://doi.org/10.5194/egusphere-2026-1165
Preprint. Discussion started: 6 May 2026

- There is no nudging in the upper stratosphere, allowing the SAO to evolve freely.
- The nudging timescale is 5 days (SNAPSI uses 6 hours).

Figure 1 provides a comparison of the spatial variation of nudging timescale (i.e., of the nudging regions) in the QBOi and SNAPSI experiments.

Appendix B: Forcings and boundary conditions

CMIP6-era forcings are available from the input4MIPs website[4]. There is some flexibility in specifying forcings, at modellers' discretions, if it is reasonable to expect that minor variations will not have an important effect on the experiment results. However it is essential that the same forcings are used for all experiments that are run by the same model.

Ocean: AMIP boundary conditions for observed sea-surface temperature (SST) and sea ice (SI) can be obtained from input4MIPS, whose version `v20220201` of monthly `tosbcs` and siconcbcs covers the required 1979–2020 time period:

`tosbcs_input4MIPs_SSTsAndSeaIce_CMIP_PCMDI-AMIP-1-1-7_gn_187001-202106.nc`
`siconcbcs_input4MIPs_SSTsAndSeaIce_CMIP_PCMDI-AMIP-1-1-7_gn_187001-202106.nc`

Ozone: Models without interactive ozone can use their preferred ozone forcing that is suitable for the historical period. This can be climatological (time variation is only seasonal) or transient (time variation can also include trends or other variability). While transient ozone may be most consistent with the transient SST/SI boundary conditions, modellers should not use prescribed ozone that already contains a QBO signal, since this can influence the evolution of a model's spontaneous QBO (Butchart et al., 2023) and thus affect the results of Exp1. For example, the CMIP historical-era ozone forcing available at the input4MIPs

`vmro3_input4MIPs_ozone_CMIP_UReading-CCMI-1-0_gn_*.nc`

contains a QBO signal and therefore should be avoided.

Volcanoes: For consistency with the prescribed QBO and ocean boundary conditions, volcanic aerosol forcing is corresponding to historical eruptions in the 1979–2020 period is recommended. However, given uncertainties in the QBO response to volcanic forcing, this is not considered essential.

11-year solar cycle: Similarly to volcanoes, a prescribed 11-year solar cycle in solar total irradiance and UV irradiance is recommended but not required.

Trace gas concentrations: Concentrations of CO_2 and other radiatively active trace gases are recommended to follow transient forcings available from input4MIPs, so as to be consistent SST/SI trends over the 1979–2020 period.

Appendix C: Data request

The QBOi phase-2 data request comprises 85 variables, as listed in Tables C1–C6. Of these, 68 were requested for the QBOi phase-1 experiments (Butchart et al., 2018). An additional 17 variables are newly requested in phase-2. These are included in

[4]https://esgf-node.llnl.gov/search/input4mips/

https://doi.org/10.5194/egusphere-2026-1165
Preprint. Discussion started: 6 May 2026

Tables C1–C6, but are also listed separately in Table C7 in order to clarify what has changed since the phase-1 data request. Each of Tables C1–C6 specifies the short name of the requested variable (used in the netcdf file and filename), its longer and more human-readable name, units, requested frequencies, and the spatial dimensions/coordinates for each requested frequency.

The Transformed-Eulerian Mean (TEM) quantities in Table C2 should be calculated using 6-hourly instantaneous samples and then averaged to daily or monthly means, consistent with the method prescribed by DynVarMIP requirements for CMIP6 output (Gerber and Manzini, 2016, including their Corrigendum). That is, eddy covariances ($\overline{u'v'}$, etc) should be computed by multiplying 6-hourly eddy quantities and then zonal averaging. All multiplicative products (i.e., multiplying eddy covariances by mean-flow terms to compute the EP flux components) should be computed at 6-hourly frequency before time averaging to daily or monthly means. These calculations are best carried out on a pressure levels grid with vertical resolution comparable to the model resolution, so as to reduce errors in the computation of vertical derivatives (Gerber and Manzini, 2016). The final results can then be interpolated to the requested standard pressure levels specified in Table C2.

Table C1. Surface and 3D circulation variables, monthly mean and daily mean. Pressure levels for 3D variables are either the 8-level plev8 grid or the 30-level qboi30 grid, as indicated.

Name	Long name	Units	Table	Spatial dimensions
pr	Precipitation	kg m-2 s-1	mon, day	longitude, latitude
prc	Convective Precipitation	kg m-2 s-1	mon, day	longitude, latitude
psl	Sea Level Pressure	Pa	mon, day	longitude, latitude
ta	Air Temperature	K	mon	longitude, latitude, qboi30
			day	longitude, latitude, plev8
tas	Near-Surface Air Temperature	K	mon, day	longitude, latitude, height2m
ua	Eastward Wind	m s-1	mon	longitude, latitude, qboi30
			day	longitude, latitude, plev8
uas	Eastward Near-Surface Wind	m s-1	mon, day	longitude, latitude, height10m
va	Northward Wind	m s-1	mon	longitude, latitude, qboi30
			day	longitude, latitude, plev8
vas	Northward Near-Surface Wind	m s-1	mon, day	longitude, latitude, height10m
zg	Geopotential Height	m	mon	longitude, latitude, qboi30
			day	longitude, latitude, plev8

Author contributions. The protocol was initially designed by JAA, NB, SO, YK, KH, TS, and JHR. JAA, NB, and SO contributed to the text and figures of the paper. The remaining authors provided input to the experimental design, provided model out and reviewed and edited the manuscript.

https://doi.org/10.5194/egusphere-2026-1165
Preprint. Discussion started: 6 May 2026

Table C2. Zonal-mean quantities, including Transformed-Eulerian Mean (TEM) momentum budget terms, monthly mean and daily mean.

Name	Long name	Units	Table	Spatial dimensions
epfy	Northward Component of the Eliassen-Palm Flux	m3 s-2	monZ, dayZ	latitude, qboi30
epfz	Upward Component of the Eliassen-Palm Flux	m3 s-2	monZ, dayZ	latitude, qboi30
psitem	Transformed Eulerian Mean Mass Streamfunction	kg s-1	monZ, dayZ	latitude, qboi30
ta	Air Temperature	K	monZ, dayZ	latitude, qboi30
ua	Eastward Wind	m s-1	monZ, dayZ	latitude, qboi30
utendepfd	Tendency of Eastward Wind Due to Eliassen-Palm Flux Divergence	m s-2	monZ, dayZ	latitude, qboi30
utendmp	Tendency of Eastward Wind Due to Model Physics	m s-2	monZ, dayZ	latitude, qboi30
utendnd	Tendency of Eastward Wind Due to Imposed Relaxation	m s-2	monZ, dayZ	latitude, qboi30
utendnogw	Eastward Acceleration Due to Non-Orographic Gravity Wave Drag	m s-2	monZ, dayZ	latitude, qboi30
utendogw	Eastward Acceleration Due to Orographic Gravity Wave Drag	m s-2	monZ, dayZ	latitude, qboi30
utendvtem	Tendency of Eastward Wind Due to TEM Northward Advection and Coriolis Term	m s-2	monZ, dayZ	latitude, qboi30
utendwtem	Tendency of Eastward Wind Due to TEM Upward Advection	m s-2	monZ, dayZ	latitude, qboi30
vtem	Transformed Eulerian Mean Northward Wind	m s-1	monZ, dayZ	latitude, qboi30
wtem	Transformed Eulerian Mean Upward Wind	m s-1	monZ, dayZ	latitude, qboi30
zg	Geopotential Height	m	monZ, dayZ	latitude, qboi30

Table C3. Zonally varying gravity wave sources and tendencies, monthly mean and daily mean. Launch stresses for non-orographic waves are requested at the model's launch level (which varies by model).

Name	Long name	Units	Table	Spatial dimensions
taunoge	Eastward Wind Stress Due to Non-Orographic Gravity Wave Drag	Pa	mon	longitude, latitude, qboi30
	Eastward Launch Stress Due to Non-Orographic Gravity Wave Drag		day	longitude, latitude
taunogn	Northward Wind Stress Due to Non-Orographic Gravity Wave Drag	Pa	mon	longitude, latitude, qboi30
	Northward Launch Stress Due to Non-Orographic Gravity Wave Drag		day	longitude, latitude
taunogs	Southward Wind Stress Due to Non-Orographic Gravity Wave Drag	Pa	mon	longitude, latitude, qboi30
	Southward Launch Stress Due to Non-Orographic Gravity Wave Drag		day	longitude, latitude
taunogw	Westward Wind Stress Due to Non-Orographic Gravity Wave Drag	Pa	mon	longitude, latitude, qboi30
	Westward Launch Stress Due to Non-Orographic Gravity Wave Drag		day	longitude, latitude
tauogu	Eastward Surface Stress Due to Orographic Gravity Wave Drag	Pa	day	longitude, latitude
tauogv	Northward Surface Stress Due to Orographic Gravity Wave Drag	Pa	day	longitude, latitude
utendnogw	Eastward Acceleration Due to Non-Orographic Gravity Wave Drag	m s-2	mon	longitude, latitude, qboi30
utendogw	Eastward Acceleration Due to Orographic Gravity Wave Drag	m s-2	mon	longitude, latitude, qboi30
vtendnogw	Northward Acceleration Due to Non-Orographic Gravity Wave Drag	m s-2	mon	longitude, latitude, qboi30
vtendogw	Northward Acceleration Due to Orographic Gravity Wave Drag	m s-2	mon	longitude, latitude, qboi30

https://doi.org/10.5194/egusphere-2026-1165
Preprint. Discussion started: 6 May 2026

Table C4. Constituents and thermodynamics, monthly mean and daily mean.

Name	Long name	Units	Table	Spatial dimensions
hus	Specific Humidity	kg kg-1	mon	longitude, latitude, qboi30
			monZ	latitude, qboi30
			dayZ	latitude, qboi30
o3	Mole Fraction of O3	mol mol-1	monZ, dayZ	latitude, qboi30
tntmp	Tendency of Air Temperature Due to Model Physics	K s-1	monZ, dayZ	latitude, qboi30
tntrl	Tendency of Air Temperature Due to Longwave Radiative Heating	K s-1	monZ, dayZ	latitude, qboi30
tntrs	Tendency of Air Temperature Due to Shortwave Radiative Heating	K s-1	monZ, dayZ	latitude, qboi30

Table C5. Circulation variables for analysis of equatorial waves (spectral analysis), 6-hourly instantaneous samples. These 3D variables are requested on a pressure levels grid spanning the 150–0.4 hPa ($\sim$ 13–54 km) range, for which the pressures are a good approximation to a model's actual vertical levels. Hence the exact pressures will depend on the model, but the resulting grid is referred to in the data request as qboiplevm. The lowermost requested altitude of 150 hPa ($\sim$ 13 km) differs from the lowermost requested altitude of 100 hPa ($\sim$ 16 km) in Butchart et al. (2018), following Kawatani et al. (2025). Horizontal resolution should be at or as close as possible to the model's actual resolution. These variables may be provided in a 15°S–15°N channel to reduce data volume.

Name	Long name	Units	Table	Spatial dimensions
ta	Air Temperature	K	6hrPt	longitude, latitude, qboiplevm
ua	Eastward Wind	m s-1	6hrPt	longitude, latitude, qboiplevm
va	Northward Wind	m s-1	6hrPt	longitude, latitude, qboiplevm
wap	Omega (=dp/dt)	Pa s-1	6hrPt	longitude, latitude, qboiplevm

Competing interests. The authors declare no competing interests.

Acknowledgements. We gratefully acknowledge support for the QBOi activity from the Atmospheric Processes And their Role in Climate (APARC; https://www.sparc-climate.org/) core project of the World Climate Research Programme (WCRP; https://www.wcrp-climate.org/). We also gratefully acknowledge the UK Centre for Environmental Data Analysis (CEDA; https://www.ceda.ac.uk/) for hosting the QBOi data archive and providing computing resources via the JASMIN platform (https://jasmin.ac.uk/). MBA, NB, and JK were funded by the Met Office Climate Science for Service Partnership (CSSP) China project under the International Science Partnerships Fund (ISPF). We acknowledge use of the Monsoon2 system, a collaborative facility supplied under the Joint Weather and Climate Research Programme, a strategic partnership between the Met Office and the Natural Environment Research Council, to perform some of the HadGEM3GA7.1 simulations. The EC-Earth3 simulations were performed thanks to ECMWF's computing and archive facilities made available through an ECMWF Special Project. YL was supported by the National Natural Science Foundation of China (Grant no. 42275056). SWS and DCH were supported by the National Research Foundation of Korea (NRF) grant funded by the Korea government (MSIT)(RS-2025-02363044) ZC was funded by the National Natural Science Foundation of China (42405170) and the Chinese Academy of Sciences Key Scientific Research Project

https://doi.org/10.5194/egusphere-2026-1165
Preprint. Discussion started: 6 May 2026

Table C6. Variables for analysis of the Madden-Julian Oscillation (MJO).

Name	Long name	Units	Table	Spatial dimensions
pr	Precipitation	kg m-2 s-1	3hr	longitude, latitude
rlut	TOA Outgoing Longwave Radiation	W m-2	day, 3hr	longitude, latitude
ua200	Eastward Wind	m s-1	day	longitude, latitude, p200
va200	Northward Wind	m s-1	day	longitude, latitude, p200
va850	Northward Wind	m s-1	day	longitude, latitude, p850

Table C7. Summary of variables added in QBOi phase-2. These variables were not part of the QBOi phase-1 data request described by Butchart et al. (2018). All of these variable have already been included in Tables C1–C6, but are summarized here for the convenience of modellers who have already implemented the phase-1 request. An additional change from the phase-1 request is that the lowermost requested altitude for variables in Table C5 (equatorial wave analysis) is 150 hPa ($\sim$ 13 km) instead of 100 hPa ($\sim$ 16 km) as in Butchart et al. (2018).

Name	Long name	Units	Table	Spatial dimensions
hus	Specific Humidity	kg kg-1	mon	longitude, latitude, qboi30
pr	Precipitation	kg m-2 s-1	3hr	longitude, latitude
rlut	TOA Outgoing Longwave Radiation	W m-2	day, 3hr	longitude, latitude
ua200	Eastward Wind	m s-1	day	longitude, latitude, p200
utendmp	Tendency of Eastward Wind Due to Model Physics	m s-2	monZ, dayZ	latitude, qboi30
utendnd	Tendency of Eastward Wind Due to Imposed Relaxation	m s-2	monZ, dayZ	latitude, qboi30
utendvtem	Tendency of Eastward Wind Due to TEM Northward Advection and Coriolis Term	m s-2	monZ, dayZ	latitude, qboi30
utendwtem	Tendency of Eastward Wind Due to TEM Upward Advection	m s-2	monZ, dayZ	latitude, qboi30
va	Northward Wind	m s-1	mon day	longitude, latitude, qboi30 longitude, latitude, plev8
va200	Northward Wind	m s-1	day	longitude, latitude, p200
va850	Northward Wind	m s-1	day	longitude, latitude, p850

(KGFZD-145-24-33), and was technically supported by the National Large Scientific and Technological Infrastructure—Earth System Numerical Simulation Facility in China (https://cstr.cn/31134.02.EL). SW and YK were supported by the MEXT Program for Advanced Studies of Climate Change Projection (SENTAN) under Grant Number JPMXD0722681344 and by the Japan Society for the Promotion of Science (JSPS) through a Grant-in-Aid for Scientific Research (Grant Number JP22H01303 and JP23K22574). The MIROC6.1 simulations were performed using the Earth Simulator at the Japan Agency for Marine-Earth Science and Technology (JAMSTEC).

https://doi.org/10.5194/egusphere-2026-1165
Preprint. Discussion started: 6 May 2026

References

Alexander, M. J. and Dunkerton, T. J.: A Spectral Parameterization of Mean-Flow Forcing due to Breaking Gravity Waves, Journal of the Atmospheric Sciences, 56, 4167 – 4182, https://doi.org/10.1175/1520-0469(1999)056<4167:ASPOMF>2.0.CO;2, 1999.

Alexander, M. J., Liu, C. C., Bacmeister, J., Bramberger, M., Hertzog, A., and Richter, J. H.: Observational Validation of Parameterized Gravity Waves From Tropical Convection in the Whole Atmosphere Community Climate Model, Journal of Geophysical Research: Atmospheres, 126, e2020JD033 954, https://doi.org/https://doi.org/10.1029/2020JD033954, e2020JD033954 2020JD033954, 2021.

Andrews, D. G., Holton, J. R., and Leovy, C. B.: Middle Atmosphere Dynamics, Academic, San Diego, Calif., 1987.

Andrews, M. B., Butchart, N., Anstey, J. A., Bednarz, E., Elsbury, D., García-Franco, J. L., Kumar, V., Palmeiro, F. M., Trencham, N. E., Yoshida, K., Chai, Z., Hong, D.-C., Huang, K., Jaison, A. M., Kawatani, Y., Knight, J. R., Lin, P., Lott, F., Lu, Y., Naoe, H., Osprey, S. M., Richter, J. H., Serva, F., Son, S.-W., Tang, Q., Watanabe, S., and Xie, J.: Extratropical teleconnections in a multi-model ensemble nudged towards the observed QBO, EGUsphere, 2026, 1–33, https://doi.org/10.5194/egusphere-2026-737, 2026.

Anstey, J. A. and Shepherd, T. G.: High-latitude influence of the quasi-biennial oscillation, Quarterly Journal of the Royal Meteorological Society, 140, 1–21, https://doi.org/10.1002/qj.2132, 2014.

Anstey, J. A., Scinocca, J. F., and Keller, M.: Simulating the QBO in an Atmospheric General Circulation Model: Sensitivity to Resolved and Parameterized Forcing, Journal of the Atmospheric Sciences, 73, 1649 – 1665, https://doi.org/10.1175/JAS-D-15-0099.1, 2016.

Anstey, J. A., Banyard, T. P., Butchart, N., Coy, L., Newman, P. A., Osprey, S., and Wright, C. J.: Prospect of increased disruption to the QBO in a changing climate, Geophysical Research Letters, 48, e2021GL093 058, https://doi.org/https://doi.org/10.1029/2021GL093058, 2021.

Anstey, J. A., Butchart, N., Hamilton, K., and Osprey, S. M.: The SPARC Quasi-Biennial Oscillation initiative, Quarterly Journal of the Royal Meteorological Society, 148, 1455–1458, https://doi.org/https://doi.org/10.1002/qj.3820, 2022a.

Anstey, J. A., Simpson, I. R., Richter, J. H., Naoe, H., Taguchi, M., Serva, F., Gray, L. J., Butchart, N., Hamilton, K., Osprey, S., Bellprat, O., Braesicke, P., Bushell, A. C., Cagnazzo, C., Chen, C.-C., Chun, H.-Y., Garcia, R. R., Holt, L., Kawatani, Y., Kerzenmacher, T., Kim, Y.-H., Lott, F., McLandress, C., Scinocca, J., Stockdale, T. N., Versick, S., Watanabe, S., Yoshida, K., and Yukimoto, S.: Teleconnections of the Quasi-Biennial Oscillation in a multi-model ensemble of QBO-resolving models, Quarterly Journal of the Royal Meteorological Society, 148, 1568–1592, https://doi.org/https://doi.org/10.1002/qj.4048, 2022b.

Arakawa, A. and Schubert, W. H.: Interaction of a Cumulus Cloud Ensemble with the Large-Scale Environment, Part I, Journal of Atmospheric Sciences, 31, 674 – 701, https://doi.org/10.1175/1520-0469(1974)031<0674:IOACCE>2.0.CO;2, 1974.

Baldwin, M. P., Gray, L. J., Dunkerton, T. J., Hamilton, K., Haynes, P. H., Randel, W. J., Holton, J. R., Alexander, M. J., Hirota, I., Horinouchi, T., Jones, D. B. a., Kinnersley, J. S., Marquardt, C., Sato, K., and Takahashi, M.: The quasi-biennial oscillation, Reviews of Geophysics, 39, 179–229, https://doi.org/10.1029/1999RG000073, 2001.

Bechtold, P., Semane, N., Lopez, P., Chaboureau, J.-P., Beljaars, A., and Bormann, N.: Representing Equilibrium and Nonequilibrium Convection in Large-Scale Models, Journal of the Atmospheric Sciences, 71, 734 – 753, https://doi.org/10.1175/JAS-D-13-0163.1, 2014.

Beres, J. H., Alexander, M. J., and Holton, J. R.: A Method of Specifying the Gravity Wave Spectrum above Convection Based on Latent Heating Properties and Background Wind, Journal of the Atmospheric Sciences, 61, 324 – 337, https://doi.org/10.1175/1520-0469(2004)061<0324:AMOSTG>2.0.CO;2, 2004.

https://doi.org/10.5194/egusphere-2026-1165
Preprint. Discussion started: 6 May 2026

Bramberger, M., Goetz, D., Alexander, M. J., Kalnajs, L., Hertzog, A., and Podglajen, A.: Tropical Wave Observations From the Reel-Down Atmospheric Temperature Sensor (RATS) in the Lowermost Stratosphere During Strateole-2, Geophysical Research Letters, 50, e2023GL104 711, https://doi.org/https://doi.org/10.1029/2023GL104711, e2023GL104711 2023GL104711, 2023.

Bushell, A. C., Butchart, N., Derbyshire, S. H., Jackson, D. R., Shutts, G. J., Vosper, S. B., and Webster, S.: Parameterized Gravity Wave Momentum Fluxes from Sources Related to Convection and Large-Scale Precipitation Processes in a Global Atmosphere Model, Journal of the Atmospheric Sciences, 72, 4349 – 4371, https://doi.org/10.1175/JAS-D-15-0022.1, 2015.

Bushell, A. C., Anstey, J. A., Butchart, N., Kawatani, Y., Osprey, S. M., Richter, J. H., Serva, F., Braesicke, P., Cagnazzo, C., Chen, C.-C., Chun, H.-Y., Garcia, R. R., Gray, L. J., Hamilton, K., Kerzenmacher, T., Kim, Y.-H., Lott, F., McLandress, C., Naoe, H., Scinocca, J., Smith, A. K., Stockdale, T. N., Versick, S., Watanabe, S., Yoshida, K., and Yukimoto, S.: Evaluation of the Quasi-Biennial Oscillation in global climate models for the SPARC QBO-initiative, Quarterly Journal of the Royal Meteorological Society, 148, 1459–1489, https://doi.org/https://doi.org/10.1002/qj.3765, 2022.

Butchart, N.: The stratosphere: a review of the dynamics and variability, Weather and Climate Dynamics, 3, 1237–1272, https://doi.org/10.5194/wcd-3-1237-2022, 2022.

Butchart, N. and Anstey, J. A.: Quasi-Biennial Oscillation, in: Reference Module in Earth Systems and Environmental Sciences, Elsevier, https://doi.org/https://doi.org/10.1016/B978-0-323-96026-7.00083-7, 2024.

Butchart, N., Scaife, A. A., Austin, J., Hare, S. H. E., and Knight, J. R.: Quasi-biennial oscillation in ozone in a coupled chemistry-climate model, Journal of Geophysical Research: Atmospheres, 108, https://doi.org/https://doi.org/10.1029/2002JD003004, 2003.

Butchart, N., Anstey, J. A., Hamilton, K., Osprey, S., McLandress, C., Bushell, A. C., Kawatani, Y., Kim, Y.-H., Lott, F., Scinocca, J., Stockdale, T. N., Andrews, M., Bellprat, O., Braesicke, P., Cagnazzo, C., Chen, C.-C., Chun, H.-Y., Dobrynin, M., Garcia, R. R., Garcia-Serrano, J., Gray, L. J., Holt, L., Kerzenmacher, T., Naoe, H., Pohlmann, H., Richter, J. H., Scaife, A. A., Schenzinger, V., Serva, F., Versick, S., Watanabe, S., Yoshida, K., and Yukimoto, S.: Overview of experiment design and comparison of models participating in phase 1 of the SPARC Quasi-Biennial Oscillation initiative (QBOi), Geoscientific Model Development, 11, 1009–1032, https://doi.org/10.5194/gmd-11-1009-2018, 2018.

Butchart, N., Andrews, M. B., and Jones, C. D.: QBO Phase Synchronization in CMIP6 Historical Simulations Attributed to Ozone Forcing, Geophysical Research Letters, 50, e2023GL104 401, https://doi.org/https://doi.org/10.1029/2023GL104401, e2023GL104401 2023GL104401, 2023.

Chai, Z., Zhang, M., Zeng, Q., Xie, J., You, T., and Zhang, H.: Simulation of the QBO in IAP-AGCM: Analysis of momentum budget: IAP-AGCMQBO, Atmospheric and Oceanic Science Letters, 14, 100 021, https://doi.org/https://doi.org/10.1016/j.aosl.2020.100021, 2021.

Charron, M. and Manzini, E.: Gravity Waves from Fronts: Parameterization and Middle Atmosphere Response in a General Circulation Model, Journal of the Atmospheric Sciences, 59, 923 – 941, https://doi.org/10.1175/1520-0469(2002)059<0923:GWFFPA>2.0.CO;2, 2002.

Chikira, M. and Sugiyama, M.: A Cumulus Parameterization with State-Dependent Entrainment Rate. Part I: Description and Sensitivity to Temperature and Humidity Profiles, Journal of the Atmospheric Sciences, 67, 2171 – 2193, https://doi.org/10.1175/2010JAS3316.1, 2010.

Coy, L., Wargan, K., Molod, A. M., McCarty, W. R., and Pawson, S.: Structure and Dynamics of the Quasi-Biennial Oscillation in MERRA-2, Journal of Climate, 29, 5339–5354, https://doi.org/10.1175/JCLI-D-15-0809.1, 2016.

Dall'Amico, M., Gray, L. J., Rosenlof, K. H., Scaife, A. A., Shine, K. P., and Stott, P. A.: Stratospheric temperature trends: impact of ozone variability and the QBO, Clim. Dyn., 34, 381–398, 2010.

https://doi.org/10.5194/egusphere-2026-1165
Preprint. Discussion started: 6 May 2026

Danabasoglu, G., Lamarque, J.-F., Bacmeister, J., Bailey, D. A., DuVivier, A. K., Edwards, J., Emmons, L. K., Fasullo, J., Garcia, R., Gettelman, A., Hannay, C., Holland, M. M., Large, W. G., Lauritzen, P. H., Lawrence, D. M., Lenaerts, J. T. M., Lindsay, K., Lipscomb, W. H., Mills, M. J., Neale, R., Oleson, K. W., Otto-Bliesner, B., Phillips, A. S., Sacks, W., Tilmes, S., van Kampenhout, L., Vertenstein, M., Bertini, A., Dennis, J., Deser, C., Fischer, C., Fox-Kemper, B., Kay, J. E., Kinnison, D., Kushner, P. J., Larson, V. E., Long, M. C., Mickelson, S., Moore, J. K., Nienhouse, E., Polvani, L., Rasch, P. J., and Strand, W. G.: The Community Earth System Model Version 2 (CESM2), Journal of Advances in Modeling Earth Systems, 12, e2019MS001 916, https://doi.org/10.1029/2019MS001916, e2019MS001916 2019MS001916, 2020.

de la Cámara, A. and Lott, F.: A parameterization of gravity waves emitted by fronts and jets, Geophysical Research Letters, 42, 2071–2078, https://doi.org/https://doi.org/10.1002/2015GL063298, 2015.

Döscher, R., Acosta, M., Alessandri, A., Anthoni, P., Arsouze, T., Bergman, T., Bernardello, R., Boussetta, S., Caron, L.-P., Carver, G., Castrillo, M., Catalano, F., Cvijanovic, I., Davini, P., Dekker, E., Doblas-Reyes, F. J., Docquier, D., Echevarria, P., Fladrich, U., Fuentes-Franco, R., Gröger, M., v. Hardenberg, J., Hieronymus, J., Karami, M. P., Keskinen, J.-P., Koenigk, T., Makkonen, R., Massonnet, F., Ménégoz, M., Miller, P. A., Moreno-Chamarro, E., Nieradzik, L., van Noije, T., Nolan, P., O'Donnell, D., Ollinaho, P., van den Oord, G., Ortega, P., Prims, O. T., Ramos, A., Reerink, T., Rousset, C., Ruprich-Robert, Y., Le Sager, P., Schmith, T., Schrödner, R., Serva, F., Sicardi, V., Sloth Madsen, M., Smith, B., Tian, T., Tourigny, E., Uotila, P., Vancoppenolle, M., Wang, S., Wårlind, D., Willén, U., Wyser, K., Yang, S., Yepes-Arbós, X., and Zhang, Q.: The EC-Earth3 Earth system model for the Coupled Model Intercomparison Project 6, Geoscientific Model Development, 15, 2973–3020, https://doi.org/10.5194/gmd-15-2973-2022, 2022.

Dunkerton, T. J.: The role of gravity waves in the quasi-biennial oscillation, Journal of Geophysical Research: Atmospheres, 102, 26 053–26 076, https://doi.org/https://doi.org/10.1029/96JD02999, 1997.

Dunkerton, T. J. and Delisi, D. P.: Climatology of the Equatorial Lower Stratosphere, Journal of the Atmospheric Sciences, 42, 376–396, https://doi.org/10.1175/1520-0469(1985)042<0376:COTELS>2.0.CO;2, 1985.

Elsbury, D., Serva, F., Caron, J. M., Back, S.-Y., Orbe, C., Richter, J. H., Anstey, J. A., Butchart, N., Chen, C.-C., García-Serrano, J., Glanville, A., Kawatani, Y., Kerzenmacher, T., Lott, F., Naoe, H., Osprey, S., Palmeiro, F. M., Son, S.-W., Taguchi, M., Versick, S., Watanabe, S., and Yoshida, K.: QBOi El Niño Southern Oscillation experiments: Assessing relationships between ENSO, MJO, and QBO, EGUsphere, 2025, 1–35, https://doi.org/10.5194/egusphere-2024-3950, 2025.

Emori, S., Nozawa, T., Numaguti, A., and Uno, I.: Importance of Cumulus Parameterization for Precipitation Simulation over East Asia in June, Journal of the Meteorological Society of Japan. Ser. II, 79, 939–947, https://doi.org/10.2151/jmsj.79.939, 2001.

Eyring, V., Bony, S., Meehl, G. A., Senior, C. A., Stevens, B., Stouffer, R. J., and Taylor, K. E.: Overview of the Coupled Model Intercomparison Project Phase 6 (CMIP6) experimental design and organization, Geoscientific Model Development, 9, 1937–1958, https://doi.org/10.5194/gmd-9-1937-2016, 2016.

Fujiwara, M., Manney, G. L., Gray, L. J., and Wright, J. S. E.: SPARC Reanalysis Intercomparison Project (S-RIP) Final Report, Tech. rep., https://doi.org/10.17874/800dee57d13, 2022.

Garfinkel, C. I., Gerber, E. P., Shamir, O., Rao, J., Jucker, M., White, I., and Paldor, N.: A QBO Cookbook: Sensitivity of the Quasi-Biennial Oscillation to Resolution, Resolved Waves, and Parameterized Gravity Waves, Journal of Advances in Modeling Earth Systems, 14, e2021MS002 568, https://doi.org/https://doi.org/10.1029/2021MS002568, e2021MS002568 2021MS002568, 2022.

Geller, M. A., Zhou, T., Shindell, D., Ruedy, R., Aleinov, I., Nazarenko, L., Tausnev, N. L., Kelley, M., Sun, S., Cheng, Y., Field, R. D., and Faluvegi, G.: Modeling the QBO—Improvements resulting from higher-model vertical resolution, Journal of Advances in Modeling Earth Systems, 8, 1092–1105, https://doi.org/https://doi.org/10.1002/2016MS000699, 2016.

https://doi.org/10.5194/egusphere-2026-1165
Preprint. Discussion started: 6 May 2026

Gerber, E. P. and Manzini, E.: The Dynamics and Variability Model Intercomparison Project (DynVarMIP) for CMIP6: assessing the stratosphere–troposphere system, Geoscientific Model Development, 9, 3413–3425, https://doi.org/10.5194/gmd-9-3413-2016, 2016.

Golaz, J.-C., Van Roekel, L. P., Zheng, X., Roberts, A. F., Wolfe, J. D., Lin, W., Bradley, A. M., Tang, Q., Maltrud, M. E., Forsyth, R. M., Zhang, C., Zhou, T., Zhang, K., Zender, C. S., Wu, M., Wang, H., Turner, A. K., Singh, B., Richter, J. H., Qin, Y., Petersen, M. R., Mametjanov, A., Ma, P.-L., Larson, V. E., Krishna, J., Keen, N. D., Jeffery, N., Hunke, E. C., Hannah, W. M., Guba, O., Griffin, B. M., Feng, Y., Engwirda, D., Di Vittorio, A. V., Dang, C., Conlon, L. M., Chen, C.-C.-J., Brunke, M. A., Bisht, G., Benedict, J. J., Asay-Davis, X. S., Zhang, Y., Zhang, M., Zeng, X., Xie, S., Wolfram, P. J., Vo, T., Veneziani, M., Tesfa, T. K., Sreepathi, S., Salinger, A. G., Reeves Eyre, J. E. J., Prather, M. J., Mahajan, S., Li, Q., Jones, P. W., Jacob, R. L., Huebler, G. W., Huang, X., Hillman, B. R., Harrop, B. E., Foucar, J. G., Fang, Y., Comeau, D. S., Caldwell, P. M., Bartoletti, T., Balaguru, K., Taylor, M. A., McCoy, R. B., Leung, L. R., and Bader, D. C.: The DOE E3SM Model Version 2: Overview of the Physical Model and Initial Model Evaluation, Journal of Advances in Modeling Earth Systems, 14, e2022MS003 156, https://doi.org/https://doi.org/10.1029/2022MS003156, e2022MS003156 2022MS003156, 2022.

Hamilton, K.: Effects of an Imposed Quasi-Biennial Oscillation in a Comprehensive Troposphere–Stratosphere–Mesosphere General Circulation Model, Journal of the Atmospheric Sciences, 55, 2393 – 2418, https://doi.org/10.1175/1520-0469(1998)055<2393:EOAIQB>2.0.CO;2, 1998.

Hamilton, K.: On the Quasi-Decadal Modulation of the Stratospheric QBO Period, Journal of Climate, 15, 2562 – 2565, https://doi.org/10.1175/1520-0442(2002)015<2562:OTQDMO>2.0.CO;2, 2002.

Hamilton, K., Osprey, S., and Butchart, N.: Modeling the stratosphere's "heartbeat", Eos, 96, https://doi.org/doi:10.1029/2015EO032301, 2015.

Han, J.-Y., Hong, S.-Y., and Kwon, Y. C.: The Performance of a Revised Simplified Arakawa–Schubert (SAS) Convection Scheme in the Medium-Range Forecasts of the Korean Integrated Model (KIM), Weather and Forecasting, 35, 1113 – 1128, https://doi.org/10.1175/WAF-D-19-0219.1, 2020.

Hansen, F., Matthes, K., and Gray, L.: Sensitivity of stratospheric dynamics and chemistry to QBO nudging width in the chemistry–climate model WACCM, Journal of Geophysical Research: Atmospheres, 118, https://doi.org/10.1002/jgrd.50812, 2013.

Hardiman, S. C., Andrews, D. G., White, A. A., Butchart, N., and Edmond, I.: Using Different Formulations of the Transformed Eulerian Mean Equations and Eliassen–Palm Diagnostics in General Circulation Models, Journal of the Atmospheric Sciences, 67, 1983 – 1995, https://doi.org/10.1175/2010JAS3355.1, 2010.

Hardiman, S. C., Butchart, N., O'Connor, F. M., and Rumbold, S. T.: The Met Office HadGEM3-ES chemistry–climate model: evaluation of stratospheric dynamics and its impact on ozone, Geoscientific Model Development, 10, 1209–1232, https://doi.org/10.5194/gmd-10-1209-2017, 2017.

Hersbach, H., Bell, B., Berrisford, P., Hirahara, S., Horányi, A., Muñoz-Sabater, J., Nicolas, J., Peubey, C., Radu, R., Schepers, D., Simmons, A., Soci, C., Abdalla, S., Abellan, X., Balsamo, G., Bechtold, P., Biavati, G., Bidlot, J., Bonavita, M., De Chiara, G., Dahlgren, P., Dee, D., Diamantakis, M., Dragani, R., Flemming, J., Forbes, R., Fuentes, M., Geer, A., Haimberger, L., Healy, S., Hogan, R. J., Hólm, E., Janisková, M., Keeley, S., Laloyaux, P., Lopez, P., Lupu, C., Radnoti, G., de Rosnay, P., Rozum, I., Vamborg, F., Villaume, S., and Thépaut, J.-N.: The ERA5 global reanalysis, Quarterly Journal of the Royal Meteorological Society, 146, 1999–2049, https://doi.org/https://doi.org/10.1002/qj.3803, 2020.

Hersbach, H., Bell, B., Berrisford, P., Biavati, G., Horányi, A., Muñoz Sabater, J., Nicolas, J., Peubey, C., Radu, R., Rozum, I., Schepers, D., Simmons, A., Soci, C., Dee, D., and Thépaut, J.-N.: ERA5 monthly averaged data on pressure levels from 1940 to present, Copernicus Climate Change Service (C3S) Climate Data Store (CDS), https://doi.org/10.24381/cds.6860a573, 2023.

https://doi.org/10.5194/egusphere-2026-1165
Preprint. Discussion started: 6 May 2026

Hines, C. O.: Doppler spreading parametrization of gravity-wave momentum deposition in the middle atmosphere. 1. Basic formulation, J. Atmos. Sol.-Terr. Phys., 59, 371–386, 1997.

Hitchcock, P., Butler, A., Charlton-Perez, A., Garfinkel, C. I., Stockdale, T., Anstey, J., Mitchell, D., Domeisen, D. I. V., Wu, T., Lu, Y., Mastrangelo, D., Malguzzi, P., Lin, H., Muncaster, R., Merryfield, B., Sigmond, M., Xiang, B., Jia, L., Hyun, Y.-K., Oh, J., Specq, D., Simpson, I. R., Richter, J. H., Barton, C., Knight, J., Lim, E.-P., and Hendon, H.: Stratospheric Nudging And Predictable Surface Impacts (SNAPSI): a protocol for investigating the role of stratospheric polar vortex disturbances in subseasonal to seasonal forecasts, Geoscientific Model Development, 15, 5073–5092, https://doi.org/10.5194/gmd-15-5073-2022, 2022.

Holt, L. A., Lott, F., Garcia, R. R., Kiladis, G. N., Cheng, Y.-M., Anstey, J. A., Braesicke, P., Bushell, A. C., Butchart, N., Cagnazzo, C., Chen, C.-C., Chun, H.-Y., Kawatani, Y., Kerzenmacher, T., Kim, Y.-H., McLandress, C., Naoe, H., Osprey, S., Richter, J. H., Scaife, A. A., Scinocca, J., Serva, F., Versick, S., Watanabe, S., Yoshida, K., and Yukimoto, S.: An evaluation of tropical waves and wave forcing of the QBO in the QBOi models, Quarterly Journal of the Royal Meteorological Society, 148, 1541–1567, https://doi.org/https://doi.org/10.1002/qj.3827, 2022.

Hood, L. L., Trencham, N. E., and Galarneau Jr, T. J.: QBO/Solar Influences on the Tropical Madden-Julian Oscillation: A Mechanism Based on Extratropical Wave Forcing in Late Fall and Early Winter, Journal of Geophysical Research: Atmospheres, 128, e2022JD037 824, https://doi.org/https://doi.org/10.1029/2022JD037824, e2022JD037824 2022JD037824, 2023.

Horowitz, L. W., Naik, V., Paulot, F., Ginoux, P. A., Dunne, J. P., Mao, J., Schnell, J., Chen, X., He, J., John, J. G., Lin, M., Lin, P., Malyshev, S., Paynter, D., Shevliakova, E., and Zhao, M.: The GFDL Global Atmospheric Chemistry-Climate Model AM4.1: Model Description and Simulation Characteristics, Journal of Advances in Modeling Earth Systems, 12, e2019MS002 032, https://doi.org/https://doi.org/10.1029/2019MS002032, e2019MS002032 2019MS002032, 2020.

Hoskins, B.: The potential for skill across the range of the seamless weather-climate prediction problem: a stimulus for our science, Quarterly Journal of the Royal Meteorological Society, 139, 573–584, https://doi.org/10.1002/qj.1991, 2013.

Hourdin, F., Rio, C., Grandpeix, J.-Y., Madeleine, J.-B., Cheruy, F., Rochetin, N., Jam, A., Musat, I., Idelkadi, A., Fairhead, L., Foujols, M.-A., Mellul, L., Traore, A.-K., Dufresne, J.-L., Boucher, O., Lefebvre, M.-P., Millour, E., Vignon, E., Jouhaud, J., Diallo, F. B., Lott, F., Gastineau, G., Caubel, A., Meurdesoif, Y., and Ghattas, J.: LMDZ6A: The Atmospheric Component of the IPSL Climate Model With Improved and Better Tuned Physics, Journal of Advances in Modeling Earth Systems, 12, e2019MS001 892, https://doi.org/https://doi.org/10.1029/2019MS001892, e2019MS001892 10.1029/2019MS001892, 2020.

Kawatani, Y., Hamilton, K., Miyazaki, K., Fujiwara, M., and Anstey, J. A.: Representation of the tropical stratospheric zonal wind in global atmospheric reanalyses, Atmospheric Chemistry and Physics, 16, 6681–6699, https://doi.org/10.5194/acp-16-6681-2016, 2016.

Kawatani, Y., Hamilton, K., Watanabe, S., Taguchi, M., Serva, F., Anstey, J. A., Richter, J. H., Butchart, N., Orbe, C., Osprey, S. M., Naoe, H., Elsbury, D., Chen, C.-C., García-Serrano, J., Glanville, A., Kerzenmacher, T., Lott, F., Palmeiro, F. M., Park, M., Versick, S., and Yoshida, K.: QBOi El Niño–Southern Oscillation experiments: overview of the experimental design and ENSO modulation of the QBO, Weather and Climate Dynamics, 6, 1045–1073, https://doi.org/10.5194/wcd-6-1045-2025, 2025.

Kim, Y.-H. and Chun, H.-Y.: Momentum forcing of the quasi-biennial oscillation by equatorial waves in recent reanalyses, Atmospheric Chemistry and Physics, 15, 6577–6587, https://doi.org/10.5194/acp-15-6577-2015, 2015.

Kim, Y.-H., Kiladis, G. N., Albers, J. R., Dias, J., Fujiwara, M., Anstey, J. A., Song, I.-S., Wright, C. J., Kawatani, Y., Lott, F., and Yoo, C.: Comparison of equatorial wave activity in the tropical tropopause layer and stratosphere represented in reanalyses, Atmospheric Chemistry and Physics, 19, 10 027–10 050, https://doi.org/10.5194/acp-19-10027-2019, 2019.

https://doi.org/10.5194/egusphere-2026-1165
Preprint. Discussion started: 6 May 2026

Koo, M.-S., Song, K., Kim, J.-E. E., Son, S.-W., Chang, E.-C., Jeong, J.-H., Kim, H., Moon, B.-K., Park, R. J., Yeh, S.-W., Yoo, C., and Hong, S.-Y.: The Global/Regional Integrated Model System (GRIMs): an Update and Seasonal Evaluation, Asia-Pacific Journal of Atmospheric Sciences, 59, 113–132, https://doi.org/10.1007/s13143-022-00297-y, 2023.

Larson, V. E.: CLUBB-SILHS: A parameterization of subgrid variability in the atmosphere, arXiv preprint arXiv:1711.03675, 2017.

Lindzen, R. S.: Turbulence and stress owing to gravity wave and tidal breakdown, Journal of Geophysical Research: Oceans, 86, 9707–9714, https://doi.org/https://doi.org/10.1029/JC086iC10p09707, 1981.

Lott, F. and Guez, L.: A stochastic parameterization of the gravity waves due to convection and its impact on the equatorial stratosphere, Journal of Geophysical Research: Atmospheres, 118, 8897–8909, https://doi.org/https://doi.org/10.1002/jgrd.50705, 2013.

Lott, F., Rani, R., McLandress, C., Podglajen, A., Bushell, A., Bramberger, M., Lee, H.-K., Alexander, J., Anstey, J., Chun, H.-Y., Hertzog, A., Butchart, N., Kim, Y.-H., Kawatani, Y., Legras, B., Manzini, E., Naoe, H., Osprey, S., Plougonven, R., Pohlmann, H., Richter, J. H., Scinocca, J., García-Serrano, J., Serva, F., Stockdale, T., Versick, S., Watanabe, S., and Yoshida, K.: Comparison between non-orographic gravity-wave parameterizations used in QBOi models and Strateole 2 constant-level balloons, Quarterly Journal of the Royal Meteorological Society, 150, 3721–3736, https://doi.org/https://doi.org/10.1002/qj.4793, 2024.

Lu, Y., Wu, T., Jie, W., Scaife, A. A., Andrews, M. B., and Richter, J. H.: Variability of the Stratospheric Quasi-Biennial Oscillation and Its Wave Forcing Simulated in the Beijing Climate Center Atmospheric General Circulation Model, Journal of the Atmospheric Sciences, 77, 149 – 165, https://doi.org/10.1175/JAS-D-19-0123.1, 2020.

Martin, Z., Son, S.-W., Butler, A., Hendon, H., Kim, H., Sobel, A., Yoden, S., and Zhang, C.: The influence of the quasi-biennial oscillation on the Madden–Julian oscillation, Nature Reviews Earth & Environment, 2, https://doi.org/10.1038/s43017-021-00173-9, 2021.

Matthes, K., Marsh, D. R., Garcia, R. R., Kinnison, D. E., Sassi, F., and Walters, S.: Role of the QBO in modulating the influence of the 11 year solar cycle on the atmosphere using constant forcings, Journal of Geophysical Research: Atmospheres, 115, https://doi.org/https://doi.org/10.1029/2009JD013020, 2010.

Naoe, H., Garcia-Franco, J. L., Park, C.-H., Rodrigo, M., Palmeiro, F. M., Serva, F., Taguchi, M., Yoshida, K., Anstey, J. A., Garcia-Serrano, J., Son, S.-W., Kawatani, Y., Butchart, N., Hamilton, K., Chen, C.-C., Glanville, A., Kerzenmacher, T., Lott, F., Orbe, C., Osprey, S., Park, M., Richter, J. H., Versick, S., and Watanabe, S.: QBOi El Niño Southern Oscillation experiments: Teleconnections of the QBO, EGUsphere, 2025, 1–36, https://doi.org/10.5194/egusphere-2025-1148, 2025.

Naujokat, B.: An Update of the Observed Quasi-Biennial Oscillation of the Stratospheric Winds over the Tropics, Journal of the Atmospheric Sciences, 43, https://doi.org/10.1175/1520-0469(1986)043<1873:AUOTOQ>2.0.CO;2, 1986.

Newman, P. A., Coy, L., Pawson, S., and Lait, L. R.: The anomalous change in the QBO in 2015–2016, Geophysical Research Letters, 43, 8791–8797, https://doi.org/https://doi.org/10.1002/2016GL070373, 2016.

Orbe, C., Ming, A., Chiodo, G., Prather, M., Diallo, M., Tang, Q., Chrysanthou, A., Naoe, H., Zhou, X., Thaler, I., Elsbury, D., Bednarz, E., Wright, J. S., Match, A., Watanabe, S., Anstey, J., Kerzenmacher, T., Versick, S., Marchand, M., Li, F., and Keeble, J.: Experimental Protocol for Phase 1 of the APARC QUOCA (QUasibiennial oscillation and Ozone Chemistry interactions in the Atmosphere) Working Group, EGUsphere, 2025, 1–36, https://doi.org/10.5194/egusphere-2025-2761, 2025.

Orr, A., Bechtold, P., Scinocca, J., Ern, M., and Janiskova, M.: Improved Middle Atmosphere Climate and Forecasts in the ECMWF Model through a Nonorographic Gravity Wave Drag Parameterization, Journal of Climate, 23, 5905 – 5926, https://doi.org/10.1175/2010JCLI3490.1, 2010.

Osprey, S. M., Butchart, N., Knight, J. R., Scaife, A. A., Hamilton, K., Anstey, J. A., Schenzinger, V., and Zhang, C.: An unexpected disruption of the atmospheric quasi-biennial oscillation, Science, 353, 1424–1427, https://doi.org/10.1126/science.aah4156, 2016.

https://doi.org/10.5194/egusphere-2026-1165
Preprint. Discussion started: 6 May 2026

Park, S. and Bretherton, C. S.: The University of Washington Shallow Convection and Moist Turbulence Schemes and Their Impact on Climate Simulations with the Community Atmosphere Model, Journal of Climate, 22, 3449 – 3469, https://doi.org/10.1175/2008JCLI2557.1, 2009.

Richter, J. H., Anstey, J. A., Butchart, N., Kawatani, Y., Meehl, G. A., Osprey, S., and Simpson, I. R.: Progress in simulating the quasi-biennial oscillation in CMIP models, Journal of Geophysical Research: Atmospheres, 125, e2019JD032 362, https://doi.org/https://doi.org/10.1029/2019JD032362, 2020.

Rio, C., Grandpeix, J.-Y., Hourdin, F., Guichard, F., Couvreux, F., Lafore, J.-P., Fridlind, A., Mrowiec, A., Roehrig, R., Rochetin, N., Lefebvre, M.-P., and Idelkadi, A.: Control of deep convection by sub-cloud lifting processes: the ALP closure in the LMDZ5B general circulation model, Clim. Dyn., 40, 2271–2292, 2013.

Rodwell, M. J., Rowell, D. P., and Folland, C. K.: Oceanic forcing of the wintertime North Atlantic Oscillation and European climate, Nature, 398, 320–323, 1999.

Scaife, A. A., Butchart, N., Warner, C. D., and Swinbank, R.: Impact of a spectral gravity wave parametrization on the stratosphere in the Met Office Unified Model, J. Atmos. Sci., 59, 1473–1489, 2002.

Scaife, A. A., Baldwin, M. P., Butler, A. H., Charlton-Perez, A. J., Domeisen, D. I. V., Garfinkel, C. I., Hardiman, S. C., Haynes, P., Karpechko, A. Y., Lim, E.-P., Noguchi, S., Perlwitz, J., Polvani, L., Richter, J. H., Scinocca, J., Sigmond, M., Shepherd, T. G., Son, S.-W., and Thompson, D. W. J.: Long-range prediction and the stratosphere, Atmospheric Chemistry and Physics, 22, 2601–2623, https://doi.org/10.5194/acp-22-2601-2022, 2022.

Schenzinger, V., Osprey, S., Gray, L., and Butchart, N.: Defining metrics of the Quasi-Biennial Oscillation in global climate models, Geoscientific Model Development, 10, 2157–2168, https://doi.org/10.5194/gmd-10-2157-2017, 2017.

Serva, F., Christiansen, B., Davini, P., von Hardenberg, J., van den Oord, G., Reerink, T. J., Wyser, K., and Yang, S.: Changes in Stratospheric Dynamics Simulated by the EC-Earth Model From CMIP5 to CMIP6, Journal of Advances in Modeling Earth Systems, 16, e2023MS003 756, https://doi.org/https://doi.org/10.1029/2023MS003756, e2023MS003756 2023MS003756, 2024.

Shibata, K.: Simulations of Ozone Feedback Effects on the Equatorial Quasi-Biennial Oscillation with a Chemistry–Climate Model, Climate, 9, https://doi.org/10.3390/cli9080123, 2021.

Shibata, K. and Deushi, M.: Radiative effect of ozone on the quasi-biennial oscillation in the equatorial stratosphere, Geophysical Research Letters, 32, https://doi.org/https://doi.org/10.1029/2005GL023433, 2005.

Simpson, I. R., Garcia, R. R., Bacmeister, J. T., Lauritzen, P. H., Hannay, C., Medeiros, B., Caron, J., Danabasoglu, G., Herrington, A., Jablonowski, C., Marsh, D., Neale, R. B., Polvani, L. M., Richter, J. H., Rosenbloom, N., and Tilmes, S.: The Path Toward Vertical Grid Options for the Community Atmosphere Model Version 7: The Impact of Vertical Resolution on the QBO and Tropical Waves, Journal of Advances in Modeling Earth Systems, 17, e2025MS004 957, https://doi.org/https://doi.org/10.1029/2025MS004957, e2025MS004957 2025MS004957, 2025.

Son, S.-W., Lim, Y., Yoo, C., Hendon, H. H., and Kim, J.: Stratospheric Control of the Madden–Julian Oscillation, Journal of Climate, 30, 1909 – 1922, https://doi.org/10.1175/JCLI-D-16-0620.1, 2017.

Stockdale, T. N., Kim, Y.-H., Anstey, J. A., Palmeiro, F. M., Butchart, N., Scaife, A. A., Andrews, M., Bushell, A. C., Dobrynin, M., Garcia-Serrano, J., Hamilton, K., Kawatani, Y., Lott, F., McLandress, C., Naoe, H., Osprey, S., Pohlmann, H., Scinocca, J., Watanabe, S., Yoshida, K., and Yukimoto, S.: Prediction of the quasi-biennial oscillation with a multi-model ensemble of QBO-resolving models, Quarterly Journal of the Royal Meteorological Society, 148, 1519–1540, https://doi.org/https://doi.org/10.1002/qj.3919, 2022.

https://doi.org/10.5194/egusphere-2026-1165
Preprint. Discussion started: 6 May 2026

Tatebe, H., Ogura, T., Nitta, T., Komuro, Y., Ogochi, K., Takemura, T., Sudo, K., Sekiguchi, M., Abe, M., Saito, F., Chikira, M., Watanabe, S., Mori, M., Hirota, N., Kawatani, Y., Mochizuki, T., Yoshimura, K., Takata, K., O'ishi, R., Yamazaki, D., Suzuki, T., Kurogi, M., Kataoka, T., Watanabe, M., and Kimoto, M.: Description and basic evaluation of simulated mean state, internal variability, and climate sensitivity in MIROC6, Geoscientific Model Development, 12, 2727–2765, https://doi.org/10.5194/gmd-12-2727-2019, 2019.

Taylor, K. E., Stouffer, R. J., and Meehl, G. A.: An Overview of CMIP5 and the Experiment Design, Bulletin of the American Meteorological Society, 93, 485 – 498, https://doi.org/10.1175/BAMS-D-11-00094.1, 2012.

Tian, W., Chipperfield, M. P., Gray, L. J., and Zawodny, J. M.: Quasi-biennial oscillation and tracer distributions in a coupled chemistry-climate model, Journal of Geophysical Research: Atmospheres, 111, https://doi.org/https://doi.org/10.1029/2005JD006871, 2006.

Walters, D., Baran, A. J., Boutle, I., Brooks, M., Earnshaw, P., Edwards, J., Furtado, K., Hill, P., Lock, A., Manners, J., Morcrette, C., Mulcahy, J., Sanchez, C., Smith, C., Stratton, R., Tennant, W., Tomassini, L., Van Weverberg, K., Vosper, S., Willett, M., Browse, J., Bushell, A., Carslaw, K., Dalvi, M., Essery, R., Gedney, N., Hardiman, S., Johnson, B., Johnson, C., Jones, A., Jones, C., Mann, G., Milton, S., Rumbold, H., Sellar, A., Ujiie, M., Whitall, M., Williams, K., and Zerroukat, M.: The Met Office Unified Model Global Atmosphere 7.0/7.1 and JULES Global Land 7.0 configurations, Geoscientific Model Development, 12, 1909–1963, https://doi.org/10.5194/gmd-12-1909-2019, 2019.

Wu, T., Lu, Y., Fang, Y., Xin, X., Li, L., Li, W., Jie, W., Zhang, J., Liu, Y., Zhang, L., Zhang, F., Zhang, Y., Wu, F., Li, J., Chu, M., Wang, Z., Shi, X., Liu, X., Wei, M., Huang, A., Zhang, Y., and Liu, X.: The Beijing Climate Center Climate System Model (BCC-CSM): the main progress from CMIP5 to CMIP6, Geoscientific Model Development, 12, 1573–1600, https://doi.org/10.5194/gmd-12-1573-2019, 2019.

Yao, W. and Jablonowski, C.: Idealized Quasi-Biennial Oscillations in an Ensemble of Dry GCM Dynamical Cores, Journal of the Atmospheric Sciences, 72, 2201 – 2226, https://doi.org/10.1175/JAS-D-14-0236.1, 2015.

Yoshimura, H., Mizuta, R., and Murakami, H.: A Spectral Cumulus Parameterization Scheme Interpolating between Two Convective Updrafts with Semi-Lagrangian Calculation of Transport by Compensatory Subsidence, Monthly Weather Review, 143, 597 – 621, https://doi.org/10.1175/MWR-D-14-00068.1, 2015.

Yu, W., Hannah, W. M., Benedict, J. J., Chen, C.-C., and Richter, J. H.: Improving the QBO Forcing by Resolved Waves With Vertical Grid Refinement in E3SMv2, Journal of Advances in Modeling Earth Systems, 17, e2024MS004473, https://doi.org/https://doi.org/10.1029/2024MS004473, e2024MS004473 2024MS004473, 2025.

Yukimoto, S., Kawai, H., Koshiro, T., Oshima, N., Yoshida, K., Urakawa, S., Tsujino, H., Deushi, M., Tanaka, T., Hosaka, M., Yabu, S., Yoshimura, H., Shindo, E., Mizuta, R., Obata, A., Adachi, Y., and Ishii, M.: The Meteorological Research Institute Earth System Model Version 2.0, MRI-ESM2.0: Description and Basic Evaluation of the Physical Component, Journal of the Meteorological Society of Japan. Ser. II, 97, 931–965, https://doi.org/10.2151/jmsj.2019-051, 2019.

Zhang, G. and McFarlane, N. A.: Sensitivity of climate simulations to the parameterization of cumulus convection in the Canadian climate centre general circulation model, Atmosphere-Ocean, 33, 407–446, https://doi.org/10.1080/07055900.1995.9649539, 1995.

Zhang, H., Zhang, M., Jin, J., Fei, K., Ji, D., Wu, C., Zhu, J., He, J., Chai, Z., Xie, J., Dong, X., Zhang, D., Bi, X., Cao, H., Chen, H., Chen, K., Chen, X., Gao, X., Hao, H., Jiang, J., Kong, X., Li, S., Li, Y., Lin, P., Lin, Z., Liu, H., Liu, X., Shi, Y., Song, M., Wang, H., Wang, T., Wang, X., Wang, Z., Wei, Y., Wu, B., Xie, Z., Xu, Y., Yu, Y., Yuan, L., Zeng, Q., Zeng, X., Zhao, S., Zhou, G., and Zhu, J.: Description and Climate Simulation Performance of CAS-ESM Version 2, Journal of Advances in Modeling Earth Systems, 12, e2020MS002210, https://doi.org/https://doi.org/10.1029/2020MS002210, e2020MS002210 2020MS002210, 2020.

https://doi.org/10.5194/egusphere-2026-1165
Preprint. Discussion started: 6 May 2026

Zhang, J., Zhang, C., Zhang, K., Xu, M., Duan, J., Chipperfield, M. P., Feng, W., Zhao, S., and Xie, F.: The role of chemical processes in the quasi-biennial oscillation (QBO) signal in stratospheric ozone, Atmospheric Environment, 244, 117 906, https://doi.org/https://doi.org/10.1016/j.atmosenv.2020.117906, 2021.

Zhao, M., Golaz, J.-C., Held, I. M., Guo, H., Balaji, V., Benson, R., Chen, J.-H., Chen, X., Donner, L. J., Dunne, J. P., Dunne, K., Durachta, J., Fan, S.-M., Freidenreich, S. M., Garner, S. T., Ginoux, P., Harris, L. M., Horowitz, L. W., Krasting, J. P., Langenhorst, A. R., Liang, Z., Lin, P., Lin, S.-J., Malyshev, S. L., Mason, E., Milly, P. C. D., Ming, Y., Naik, V., Paulot, F., Paynter, D., Phillipps, P., Radhakrishnan, A., Ramaswamy, V., Robinson, T., Schwarzkopf, D., Seman, C. J., Shevliakova, E., Shen, Z., Shin, H., Silvers, L. G., Wilson, J. R., Winton, M., Wittenberg, A. T., Wyman, B., and Xiang, B.: The GFDL Global Atmosphere and Land Model AM4.0/LM4.0: 2. Model Description, Sensitivity Studies, and Tuning Strategies, Journal of Advances in Modeling Earth Systems, 10, 735–769, https://doi.org/https://doi.org/10.1002/2017MS001209, 2018.